Multi-Neuromodulator Measurements across Fronto-Striatal Network Areas of the Behaving Macaque using Solid-Phase Microextraction

Seyed-Alireza Hassani[1,2,†] , Sofia Lendor[3,†] , Ezel Boyaci[3], Janusz Pawliszyn[3,‡,] and Thilo Womelsdorf[1,2,‡,*]

1 Department of Psychology, Vanderbilt University, PMB 407817, 2301 Vanderbilt Place, Nashville TN 37240, USA
2 Department of Biology, Centre for Vision Research, York University, Toronto, Ontario M6J 1P3, Canada
3 Department of Chemistry, University of Waterloo, 200 University Avenue West, Waterloo, Ontario N2L 3G1, Canada

* Corresponding author: Thilo Womelsdorf Tel. 615-322-0070, E-mail: thilo.womelsdorf@vanderbilt.edu
† ‡ These authors contributed equally

Short title: Sensing of multiple neurotransmitters in-vivo using SPME

Author contributions:
Seyed-Alireza Hassani and Sofia Lendor together collected all data and conducted statistical analysis of the collected data. Seyed-Alireza Hassani trained and handled the animals, prepared the MRI mapping and managed sampling equipment. Sofia Lendor prepared all SPME probes and conducted all chemical analyses/quantification of collected compounds. Ezel Boyaci contributed to the preparation of SPME probes and quality control. Janusz Pawliszyn and Thilo Womelsdorf contributed to the collection of data and analyses. All authors contributed to the writing, visualization and editing of the manuscript.

Abstract

Different neuromodulators rarely act independent from each other to modify neural processes but are instead co-released, gated, or modulated. To understand this interdependence of neuromodulators and their collective influence on local circuits during different brain states, it is necessary to reliably extract local concentrations of multiple neuromodulators in vivo. Here we describe results using solid phase microextraction (SPME), a method providing sensitive, multi-neuromodulator measurements. SPME is a sampling method that is coupled with mass spectrometry to quantify collected analytes. Reliable measurements of glutamate, dopamine, acetylcholine and choline were made simultaneously within frontal cortex and striatum of two macaque monkeys (*Macaca mulatta*) during goal-directed behavior. We find glutamate concentrations several orders of magnitude higher than acetylcholine and dopamine in all brain regions. Dopamine was reliably detected in the striatum at tenfold higher concentrations than acetylcholine. Acetylcholine and choline concentrations were detected with high consistency across brain areas, within monkeys and between monkeys. These findings illustrate that SPME microprobes provide a versatile novel tool to characterize multiple neuromodulators across different brain areas in vivo to understand the interdependence and co-variation of neuromodulators during goal directed behavior. Such data will be important to better distinguish between different behavioral states and characterize dysfunctional brain states that may be evident in psychiatric disorders.

New and Noteworthy

Our manuscript reports a reliable and sensitive novel method for measuring the absolute concentrations of glutamate, acetylcholine, choline, dopamine and serotonin in brain circuits in-vivo. We show that this method reliably samples multiple neurochemicals in three brain areas simultaneously while nonhuman primates are engaged in goal directed behavior. We further describe how the methodology we describe here may be used by electrophysiologists as a low barrier to entry tool for measuring multiple neurochemicals.

Introduction

Extracellular concentrations of neuromodulators influence firing regimes, input-output relationships and neural interactions in local circuits and long-range brain networks (Marder 2012; Thiele and Bellgrove 2018), and are dysregulated in virtually all psychiatric disorders (Avery and Krichmar 2017; Millan et al. 2012). Accumulating evidence suggests that these fundamental roles of neuromodulators for circuit functioning are unlikely realized by single neuromodulators operating in isolation. Rather, neuromodulatory systems are heavily intertwined (Avery and Krichmar 2017; Gobert et al. 1998; Moehle et al. 2017), and operate simultaneously on individual cells and circuits (Arnsten et al. 2010; Hassan et al. 2015; Marder 2012; Santana et al. 2018). In each circuit, local mechanisms exert control over the release of neuromodulators from terminals of brainstem-originating projection neurons. This local control proceeds through activation of pre-synaptic glutamatergic receptors (Ghersi et al. 2003; Grilli et al. 2009; Luccini et al. 2007; Pittaluga 2016; Pittaluga et al. 2006; Wang et al. 1992). These insights suggest that an understanding of the contribution of neuromodulators to circuit functioning requires measuring, simultaneously, multiple neuromodulators in conjunction with ongoing glutamatergic neurotransmitter concentrations and action. Consistent with this conclusion single neuromodulator theories often

71 fail to account for all observable symptoms in psychiatric diseases (Bohnen et al. 2015; Halliday
72 et al. 2014; Remy et al. 2005).

73 Despite the accumulating evidence for the interdependence of neuromodulator actions, few
74 methods exist for their simultaneous measurement in vivo and across multiple brain areas (**Table**
75 **S1;** https://github.com/att-circ-contrl/SPME_paper_SI.git). Most of these existing neurochemical
76 sensing methods allowing multi-neuromodulator sampling have a barrier to entry by requiring
77 specialized equipment and trained experts preventing data collection by scientists who are
78 otherwise interested in the role of endogenous and exogenous neuroactive chemicals in cognition
79 and psychiatric disorders. Electrochemical methods such as fast scan cyclic voltammetry (FSCV)
80 and amperometry have sub-second temporal resolution, but are limited to the measurement of a
81 few compounds (Dale et al. 2005; Jacobs et al. 2010) and are challenging and not robust for wide-
82 spread in vivo application in nonhuman primates yet, although several labs have recently reported
83 success (Disney et al. 2015; König et al. 2018; Quintero et al. 2007; Schluter et al. 2014; Schwerdt
84 et al. 2017; Vartak et al. 2017; Yoshimi et al. 2015). Imaging techniques such as positron emission
85 tomography (PET) are also limited to the measurement of one or a few compounds simultaneously
86 (Fisher et al. 1995). Microdialysis (MD) paired with mass spectrometry is the most commonly
87 used method for measuring multiple neuromodulators in awake behaving animals. MD provides a
88 data collection method which is then analyzed post hoc to identify and quantify collected analytes.
89 It operates with a semi-permeable membrane which allows for the continuous collection of the
90 available extracellular neuromodulators through passive diffusion, and can even be used to locally
91 release pharmacological agents (Anderzhanova and Wotjak 2013; Buck et al. 2009; Kennedy
92 2013; Perry et al. 2009; Watson et al. 2006). However, MD does have several disadvantages. MD
93 disrupts the tissue during its initial placement of the probe or a guiding cannula resulting in

damage-induced release of neuromodulators that can last several hours before stable measurements become possible. Moreover, MD has low affinity for hydrophobic compounds and comparatively broad spatial and temporal resolution that is in the range of 200-400 μm in diameter and 10-20 minutes, respectively. These values are dependent on the surface area of the permeable membrane, the exact method of MD, flow rate, resolution of detection methods for analytes of interest, tissue tortuosity and more (Anderzhanova and Wotjak 2013; Kennedy 2013; Watson et al. 2006).

Here, we set out to address some of these limitations with a novel protocol for measuring multiple neuromodulators in vivo in discrete 20 minute intervals using probes optimized for solid phase microextraction (SPME) (Pawliszyn 2000, 2012). SPME probes are thin (200 μm) wires of arbitrary length coated with an inert porous polymeric matrix using biocompatible binder on one end where molecules with appropriate size and affinity migrate via passive diffusion and are retained by weak intermolecular interactions (*see* Methods). SPME provides an alternate method for data collection which can then be analyzed by tools such as mass spectrometers. This method has been shown to extract in neural tissue dynamic changes in dopamine (DA) and serotonin (5-HT) levels with comparable precision to MD (Cudjoe et al. 2013; Cudjoe and Pawliszyn 2014). Additionally, due to the similarity of SPME probes to commonly used microelectrodes in electrophysiological recordings, relatively minor adjustments will allow for the adaptation of conventional microelectrode driving systems for SPME use. This, combined with post collection analysis through standard chemistry facilities makes SPME an attractive and easy-to-use tool for electrophysiology labs.

SPME has the potential to be a powerful new tool to compliment the mentioned methods well suited for neurochemical profiling that spans both multiple neuromodulators as well as multiple brain regions simultaneously. Such data will allow for global observation of slow

117 neuromodulator dynamics that could better inform our hypotheses and help relate global
118 neuromodulator levels to electrophysiology and behavior.

119 Thus, the ability of SPME to report major neuromodulators as well as glutamate and GABA
120 were tested in two behaving rhesus macaques. Probes were repeatedly and simultaneously inserted
121 into two cortical regions and the striatum to observe inter-areal differences between extracellular
122 neuromodulator concentrations. We found that extracellular concentrations of glutamate,
123 dopamine, acetylcholine and choline could be reliably distinguished and differed systematically
124 between brain regions.

125 **Methods**

126 **Animals**

127 Data was collected from two 8 year-old male rhesus macaques (*Macaca mulatta*) weighing 8-12
128 kg. All animal care and experimental protocols were approved by the York University Animal
129 Care Committee and were in accordance with the Canadian Council on Animal Care guidelines.
130 Details regarding the experimental setup, recording procedures, and reconstruction of recording
131 sites have been described previously (Oemisch et al. 2015). Briefly, animals were implanted with
132 a 20 mm by 28 mm recording chamber over the frontal region of the right hemisphere guided by
133 stereotaxic coordinates (Paxinos et al. 2000) and MR images. The animals were seated in a custom
134 made primate chair and head stabilized with their eyes 65cm away from a 21' LCD monitor
135 refreshed at 85 Hz. Eye traces were collected by a video-based eye-tracking system (Eyelink 1000
136 Osgoode, Ontario, Canada, 500 Hz sampling rate). The animals were engaged in an over-trained
137 attention tasks in which they would use saccadic eye movements to acquire juice reward (**Fig S1;**
138 https://github.com/att-circ-contrl/SPME_paper_SI.git). The specifics of the task are described
139 elsewhere (Hassani et al. 2017). Both animals showed stable performance and acquired similar

140 reward volumes on all recording days. In both tasks, stimulus presentation and reward delivery
141 was controlled through MonkeyLogic (http://www.brown.edu/Research/monkeylogic/).
142
143 **SPME protocol and Fabrication of SPME Probes**
144 We provide a visual overview of the complete SPME protocol used here in **Fig S2**
145 (https://github.com/att-circ-contrl/SPME_paper_SI.git) and delineate the chemical materials, LC-
146 MS/MS analysis, and detailed quantitation of neuromodulators in the ***Supplementary Materials***
147 (https://github.com/att-circ-contrl/SPME_paper_SI.git) and in a companion paper (Lendor et al.
148 2019). All measurements used miniaturized SPME probes that were manufactured by repeated
149 dip-coating of stainless steel wires in a suspension of extracting phase in a binder. This general
150 procedure reported previously (Gómez-Ríos et al. 2017), has been modified to fit the purpose of
151 *in vivo* brain sampling (Lendor et al. 2019). The 3 mm long tip of the wire was acid-etched down
152 to approx. 100 µm to create a recession capable of accommodating thicker layer of coating without
153 significantly increasing the total probe diameter. The extracting phase was an in-house synthesized
154 hydrophilic-lipophilic balance polymer functionalized with benzenesulfonic acid to introduce
155 strong cation exchange properties (HLB-SCX). The monodispersed polymeric particles with
156 diameter of approx. 1 µm were suspended in the binder consisting of 7% polyacrylonitrile
157 dissolved in N,N-dimethylformide (w/v), ensuring the particles-to-binder ratio at 15% (w/v). The
158 extracting phase suspension was prepared one day before the probe coating, homogenized by
159 sonication and stirred at 800 rpm overnight. Several layers of coating were deposited on the
160 modified wires, resulting in total coating thickness of ≈50 µm and total probe diameter of 195 µm.
161 The average pore size of the extracting phase was measured at 1.2nm. Before the use, the probes
162 were cleaned with the mixture of methanol, acetonitrile and 2-propanol (50:25:25, v/v/v), activated

163 in the mixture of methanol and water (50:50. v/v) and sterilized in steam for 15 min at 121°C.
164 During the sampling, SPME probes were inserted into sheathing cannulas to protect the coating
165 and prevent it from extracting compounds on the way to the target brain area. The cannulas
166 underwent the same cleaning and sterilization procedure as the probes and then the lengths of both
167 components of the SPME assembly were adjusted to 60-70 and 70-80 mm for the probes and
168 cannulas, respectively.
169

170 **MRI Guided Electrophysiological Mapping of Target Tissue**

171 The anatomical coordinates of the brain regions of interest were first identified through 3 T MR
172 images. The MR images were then verified with extracellular electrophysiological recordings of
173 the target areas, which provided the gray and white matter boundaries for the cortical sites and the
174 dorsal most aspect of the head of the caudate nucleus. Tungsten microelectrodes were 200 μm
175 thick with an impedance of 1-2 MΩ. All electrodes, SPME probes and their accompanying guiding
176 cannulas were driven down into the brain and later out using software-controlled precision
177 microdrives (Neuronitek, ON, Canada). Electrodes were connected to a multichannel acquisition
178 processor (Neuralynx Digital Lynx system, Inc., Bozeman, Montana, USA) which was used for
179 data amplification, filtering and acquisition of spiking activity. Spiking activity was obtained by
180 applying a 600-8000 Hz bandpass filter, with further amplification and digitization at a 32 KHz
181 sampling rate. For every recording day, electrodes were lowered until the first detection of spiking
182 activity (indicative of gray matter) at the depth suggested by the MR images.
183

184 **SPME Sampling and Post-Processing Procedures**

185 All three SPME assemblies (example of sampling using one assembly in **Fig 1A-C**) were
186 simultaneously driven to 200 μm above the point of first spiking detection. SPME assemblies were
187 located ~1 mm away from the electrode penetration location. Then, only the SPME probes were
188 inserted 3 mm into the areas of interest. On average macaque cortical thickness is only 2 mm while
189 the head of the caudate at the point of sampling was well over 3 mm. An extraction duration of 20
190 min was selected to reflect stable extraction time profiles for all compounds of interest. The
191 kinetics of target analyte extraction, for example glutamate and dopamine, can be visualized in
192 vitro through extraction time profiles (Lendor et al. 2019) (**Fig 1D-E**). Brain homogenate was
193 spiked with known concentrations of target analytes and four replicates were collected during
194 which multiple probes were placed in the homogenate and sequentially removed at reported times
195 after initial insertion and quantified (LC-MS/MS procedure described below). These extraction
196 time profiles reflect the quantifiable concentration of collected analyte over time, which is captured
197 in sequence by a linear "kinetic" regime, a "dynamic" regime and an "equilibrium" regime over
198 extraction time. These labels are used to describe the various rates of analyte adsorption by the
199 SPME fibre, where the kinetic regime reflects the fastest adsorbtion of the target analyte, the
200 equilibrium regime reflects a period of only marginal further analyte collection and an intermediate
201 dynamic regime (Ouyang and Pawliszyn 2007). These extraction kinetics provide information
202 about the time it takes until equilibrium is reached in a concentration independent manner that is
203 helpful in estimating a lower limit for extraction times to collect quantifiable analyte
204 concentrations. After the 20 min extraction event, all SPME probes were driven back 3 mm into
205 the guiding cannulas and all SPME assemblies were withdrawn from the brain (**Fig 1A-C**). The
206 microdrives were then removed from the chamber to enable unclamping of the SPME probes, a
207 brief wash and then storage in glass vials surrounded by dry ice until placing them into a -80°C

208 freezer. One entire sampling event (one extraction in 3 different brain areas together with
209 assembling the SPME probes and cannulas, driving into and out of brain, washing and preparing
210 for storage) was performed within 50 min, except for the first sampling event in each sampling
211 day. The first sampling event, with the area identification using electrophysiology recording, was
212 performed within 75 min. The removal of the SPME microprobe from the gray matter and the
213 positioning of a new SPME microprobe in the same location limits the temporal continuity of
214 sampling. We believe that further optimizing of the SPME microprobe switching procedure with
215 e.g. pre-loaded SPME probes will allow replacing SPME fibres within 2-10 min. Alternatively,
216 SPME microprobes could be used in spatially separate but adjacent guiding tubes (separation of
217 ~300μm), which would allow to switch sampling from one to other probe without temporal delays.
218

219 **Neuromodulator detection and quantitation**

220 Detection and quantitation of neuromodulators followed previously established procedures
221 described in the **Supplementary Materials** (https://github.com/att-circ-
222 contrl/SPME_paper_SI.git). In brief, SPME probes were defrosted and desorbed in an aqueous
223 solution containing water, acetonitrile, methanol, formic acid and deuterated isotopologues of
224 target neuromodulators as internal standards (IS). Chromatographic separation of target
225 compounds was conducted as previously reported (Cudjoe and Pawliszyn 2014). Tandem mass
226 spectrometry (MS/MS) was performed with electrospray ionization with two MS/MS transitions
227 for each neuromodulator and one for each IS (Lendor et al. 2019).

228 Stock solutions of all target neuromodulators were prepared and used to generate standard
229 calibration curves and to calculate the amounts of neuromodulator extracted by each experimental
230 SPME probe. Conversion of the amount of neuromodulator extracted to in-brain concentrations

231 was done using matrix-matched external calibrations. LOD is defined as 3 times the signal
232 obtained from blank samples.
233
234 **Results**
235 During all measurements animals were engaged in a cognitively demanding task with stable
236 behavioral performance to minimize state dependent fluctuations of basal extracellular
237 concentrations of neuromodulators. Three brain regions were selected to provide a sample of
238 extracellular neuromodulatory concentrations. Two cortical regions: prefrontal cortex (PFC) area
239 8, premotor cortex (PreMC) area 6 and the head of the caudate nucleus (CD) were selected (**Fig**
240 **1F**). In 3 daily sessions, we sampled 3 times per session simultaneously from all three areas.
241 Monkey As had an additional 3 days of recording with one sample collected on each day. Overall
242 we collected and analyzed 12 probes in monkey As and 9 probes in monkey Ke. We were
243 specifically interested in major neuromodulators and neurotransmitters but successfully measured
244 other compounds such as amino acids (e.g. glutamine, taurine, phenylalanine etc) that we do not
245 discuss here.
246 To allow comparison of the SPME extraction results to those typically reported in
247 microdialysis studies, we calculated the relative change in measured concentrations across the
248 three successive sampling events per session pooled across monkeys to enhance the statistical
249 power of the analysis (**Fig 2**). Relative to the end of the first sampling event, the second and third
250 sampling events started after 40 minutes and 100 minutes respectively. We expected that the
251 variability of measurements (indexed as standard error of the median) is comparable to repeatedly
252 measured microdialysis of an identical, active brain state. We found that measured concentrations

253 did not change significantly across sampling events for any compound area combination
254 (Wilcoxon rank sum test; **Fig 2**).

255 We found that four target neurotransmitters and neuromodulators were reliably detected in
256 each animal: glutamate, dopamine, acetylcholine, and choline. Serotonin was also detected on
257 several probes but always near the limit of detection (LOD) and therefore was excluded from
258 analyses here (Lendor et al. 2019). Glutamate concentrations were several orders of magnitude
259 higher than all other observed compounds of interest in all areas and both animals. Relative to
260 glutamate, choline concentrations were >15 times lower, DA concentrations were >700 lower and
261 ACh concentrations were >8300 times lower (**Fig 3**).

262 Glutamate concentrations (across areas), measured as median ± standard error, ranged from
263 159,147 (±19,395) to 233,659 ng/mL (±33,917) in monkey As, and from 135,523 (±22,945) to
264 184,333 ng/mL (±33,516) in monkey Ke. In both monkeys, glutamate concentrations were highest
265 in the head of the caudate, which was significantly different from glutamate concentrations in the
266 premotor cortex in monkey As (kruskal-wallis test with Tukey's HSD correction, $p = 0.048$) but
267 not in monkey Ke (kruskal-wallis test with Tukey's HSD correction, $p = 0.847$, n.s.). Glutamate
268 concentrations between the caudate and PFC, as well as the PFC and premotor cortex were not
269 significantly different for either animal. Comparisons between monkeys showed no significant
270 differences between the glutamate concentrations in any of the measured areas (**Fig 3**).

271 In addition to glutamate, dopamine could be reliably detected in both monkeys in the
272 caudate at concentrations of 232 ng/mL (±47) in monkey As, and 226 ng/mL (±31) in monkey Ke.
273 These concentrations were similar between monkeys (Wilcoxon rank sum test $p = 1$, n.s.).
274 Dopamine was not found above detection limits in frontal cortex.

275 Acetylcholine measurements in the three brain areas ranged from (across areas) 25 (±2) to
276 36 ng/mL (±5) in monkey As, and from 29 (±2) to 36 ng/mL (±4) in monkey Ke. In monkey As,
277 extracellular ACh concentrations between the caudate and premotor cortex were significantly
278 different (kruskal-wallis test with Tukey's HSD correction, p = 0.008). Cortical areas were not
279 significantly different from one another (kruskal-wallis test with Tukey's HSD correction, p =
280 0.476, n.s.) nor was there a significant difference between the caudate and PFC (kruskal-wallis test
281 with Tukey's HSD correction, p = 0.145, n.s.). In monkey Ke, only one cortical region had
282 concentrations of ACh above detection limits, which approached significant difference to the
283 concentrations measured in the caudate (Wilcoxon rank sum test, p = 0.08). Measurements of
284 extracted ACh in the pre-motor cortex of monkey Ke were consistently below detection limits (**Fig**
285 **3**).

286 We also measured choline which is a main product of the enzymatic breakdown of the
287 highly regulated ACh and which is a main indicator of attentional modulation of cholinergic
288 activity in frontal cortex (Parikh et al. 2007). Choline concentrations ranged across areas from
289 2,914 (±590) to 5,078 ng/mL (±675) in monkey As, and 3,408 (±3,705) to 5,533 ng/mL (±860) in
290 monkey Ke. Choline concentrations between the caudate and premotor cortex were significantly
291 different in monkey As (kruskal-wallis test with Tukey's HSD correction, p = 0.030), but not in
292 monkey Ke (kruskal-wallis test with Tukey's HSD correction, p = 0.729, n.s.). All other area
293 comparisons were not significant for both monkeys. Comparisons of choline concentrations
294 between monkeys were not significant in any of the measured areas.

295 Overall, serotonin concentrations were not observed as reliably as the other reported
296 neurochemicals and therefore were excluded from the main analyses. However, in monkey As,
297 serotonin was observed near the LOD in the prefrontal cortex as well as the caudate in a subset of

298 probes. Within the 9 probes placed in both areas, serotonin was detected in 22% of samples (2/9
299 probes) in the prefrontal cortex and 33% of samples (3/9 probes) in the caudate nucleus. Serotonin
300 observations ranged from 149 ng/mL to 232 ng/mL with a median of 171 ng/mL (±18.5 ng/mL;
301 standard error of the median) with a LOD of 100 ng/mL. The proximity of the measurements to
302 the LOD suggest that the other probes likely collected concentrations of serotonin below the
303 detection threshold. No serotonin observations were made in monkey Ke.
304

305 **Discussion**

306 We demonstrated the reliable measurements of glutamate, dopamine, acetylcholine and choline
307 simultaneously within cortical and subcortical regions of awake and behaving macaques using
308 coated microprobes optimized for solid phase microextraction. Glutamate concentrations were
309 several orders of magnitude higher than dopamine, acetylcholine and choline across brain regions.
310 Extracellular concentrations of choline, dopamine and acetylcholine were detected at >15, >700,
311 and >8,300 times lower than glutamate respectively. Dopamine was readily detected in the caudate
312 but not observed at detectable concentrations in the cortical regions measured. Acetylcholine
313 concentrations showed a statistical trend of being different between the caudate and measured
314 cortical areas and with high consistency between monkeys. Choline concentrations, a product of
315 acetylcholine degradation as well as a precursor for its synthesis, were negatively correlated with
316 acetylcholine ($R = -0.355$; $p = 0.01$). Together, these findings provide new and rare insights about
317 the neurochemical circuit profiles during an active brain state in three areas of the primate fronto-
318 striatal network.

319 The high consistency of measured concentrations within animals, between brain areas and
320 between monkeys suggests that SPME microprobes could provide a versatile neuro-technique for

321 understanding how variations of the neurochemical milieu relate to local and long-range circuit
322 operations and ultimately cognitive functioning.
323
324 **Extracellular Concentrations of Glutamate, Dopamine, Acetylcholine and Choline.** Our
325 results revealed particularly high levels of glutamate within all measured brain regions (PFC,
326 PreMC, and CD) relative to other neuromodulators. This finding is consistent with its ubiquitous
327 role as major excitatory neurotransmitter. This holds true even in the caudate which consists
328 exclusively of GABAergic neurons, but receives glutamatergic inputs from the cortex (Haber and
329 Knutson 2010). Tonic concentrations of glutamate within the striatum have been previously
330 reported to be comparable to that of the hippocampus, prefrontal cortex and other cortical areas
331 due to glutamatergic inputs, extra-synaptic release and glial release (Ascenzo et al. 2006;
332 Moghaddam 1993; Moussawi et al. 2011). In contrast, classical neuromodulators such as DA and
333 ACh, are released in extracellular space through volume transmission where they are highly
334 regulated and may bind to receptors on multiple neurons (Santello et al. 2012; Schwartz and Javitch
335 2013; Syková 2004; Vizi 2000). This regulation may help explain the relatively low observed
336 concentrations of DA and ACh and may be a large source of extracellular choline through the
337 enzymatic breakdown of ACh.
338 Extracellular DA was measured well above the detection threshold in the striatum. In
339 combination with glutamatergic and cholinergic concentrations, our results show promise in the
340 application of SPME to further our understanding of the relationship between glutamatergic inputs
341 to the striatum and the neuromodulatory ACh and DA signals impinging on striatal circuits. Such
342 circuits are strongly involved in hypo- and hyperkinetic diseases (Halliday et al. 2014; Millan et
343 al. 2012). Dopaminergic signals did not exceed the detection threshold in either cortical regions.

344 The presence of DA in the PFC is well documented (Goldman-Rakic et al. 1990; Vijayraghavan
345 et al. 2007; Watanabe et al. 1997) and we thus conclude that DA most likely has failed to exceed
346 our detection limit. The difference between the detection success of DA in the caudate vs PFC and
347 PreM cortex may be due to differences in available DA, release concentrations and dynamics
348 (Holloway et al. 2019). A possible explanation for the lack of detectable cortical DA is the
349 susceptibility of catecholamines to oxidation. This may be partially addressed by faster coupling
350 of sample collection to quantitation by MS.

351 Few previous studies have documented ACh concentrations in vivo in non-human primates
352 due to its rapid breakdown by acetylcholinesterase and the challenges of neurochemical testing in
353 primates (Kreitzer 2009; Schwartz and Javitch 2013; Zapata et al. 2013). ACh plays a major role
354 in organizing local circuits, deployment of attention, locomotion and reward through different
355 receptors present in cortical and subcortical regions (Granger et al. 2016; Howe et al. 2017; Moehle
356 et al. 2017). It has been difficult to discern which ACh concentration corresponds to efficient
357 endogenous circuit operations. Our finding of measurements in all sampling locations except for
358 premotor cortex in monkey Ke, is therefore a promising starting point for future studies comparing
359 ACh concentrations, in conjunction with other neuromodulators, during different cognitive states.
360 The fast turn-around of ACh due to AChE however, likely leads to an underestimation of ACh
361 concentrations by SPME. Although AChE cannot traverse the porous SPME coating due to its size
362 (~7.6nm diameter), preventing any enzymatic degradation of trapped ACh, the dynamic
363 equilibration process continuously leads to a transfer of ACh out of the SPME coating following
364 the concentration gradient of the rapidly depleted ACh into the extracellular space as discussed in
365 the case of calibration in the coating approach (Alam and Pawliszyn 2016; Zhang et al. 2007a).

366 Amongst other sources, choline is created as a byproduct of ACh degradation by AChE.
367 Choline is also a precursor for the synthesis of ACh. Given this relationship, a negative correlation
368 between choline concentrations and ACh is expected which we indeed observed in our dataset.
369 Despite the difference in the measured concentrations of choline and acetylcholine, other studies
370 with similar differences have demonstrated the relationship of ACh and choline to behavior within
371 the cortex (Parikh et al. 2007). Future studies may focus on quantifying this relationship across a
372 wider range of brain states.

373 Many factors may contribute to variation in measured concentrations of neuromodulators
374 including behavioral state, the specific brain region measured and individual differences amongst
375 others. Importantly, different methods may yield different estimates of absolute extracellular
376 concentrations. For example, comparable measurements of extracellular glutamate via MD or
377 voltammetry as opposed to electrophysiological estimates can differ by orders of magnitude and
378 may be attributed to differences in probe size, or sensitivity to different sources of glutamate
379 (Moussawi et al. 2011).

380

381 **Reliable Measurement of Individual Differences of State Specific Neuromodulatory Tone.**
382 Our results suggest that SPME probes provide reliable and sensitive measurements in consecutive
383 sampling events within an experimental session and between sessions on consecutive days. These
384 results were obtained while we controlled brain states across measurement events by engaging
385 animals in a cognitive task. This experimental control could have contributed to the comparable
386 extracellular levels of neuromodulators from sample to sample within *and* between days from
387 similar brain locations (**Fig 2**) (Marder et al. 2014; McGinley et al. 2015; Reimer et al. 2014,
388 2016). The reproducibility of multiple measurements at the same anatomical location within and

389 between days suggests that the SPME penetrations did not significantly disturb tissue (Cudjoe et
390 al. 2013). This conclusion contrasts with reported experience from microdialysis measurements,
391 where the initial placement of the probe or guiding cannula causes transient measurement
392 instabilities that can require several hours of settling time before reliable, steady state
393 neuromodulator concentrations are measurable (Kodama et al. 2002, 2015, 2017; Moussawi et al.
394 2011; Watanabe et al. 1997). These waiting periods must be taken into account when designing
395 microdialysis experiments for in vivo tracking of neuromodulators during behavioral tasks in
396 awake and restrained animals. Furthermore, the reliability of observations for the reported
397 neurochemicals with SPME is extremely high and outperforms many reported microdialysis
398 studies. We present 100% reliability in reporting glutamate and choline concentrations in all brain
399 regions and subjects. Acetylcholine concentrations were reported with 100% reliability in one
400 animal and 92% (11/12 probes) in the other within the prefrontal cortex, 0% reliability (below
401 detection threshold) in one animal and 83% (10/12 probes) in the other within the premotor cortex
402 and 100% reliability in one animal and 92% (11/12 probes) in the other within the caudate.
403 Dopamine concentrations were reported with 100% reliability in both animals in the caudate and
404 were not observed above detection thresholds in the cortex.
405
406 **Qualities and Advantages of SPME.** Our results illustrate several inherent advantages of using
407 SPME to measure neurochemical profiles in brain circuits (Lendor et al. 2019). As illustrated in
408 **Table S1** (https://github.com/att-circ-contrl/SPME_paper_SI.git), SPME complements or
409 outperforms alternative techniques in various domains. Practically, the arbitrary length of the wire
410 where the SPME coating is placed allows for robust placement within the brain. The narrow
411 diameter of the SPME probe that is within the range common to electrodes for electrophysiological

412 recordings, allows for repeated, simultaneous sampling at multiple sites without observable
413 changes to detected extracellular neuromodulator levels using 20-minute sampling times.

414 *Spatial Resolution.* In principle, the spatial resolution of the SPME measurements are
415 capable of reflecting laminar concentration gradients across areas as small as several tens of
416 micrometers. In our protocol we coated 3mm in length with 50 μm of thickness and desorbed the
417 entire area into an organic solvent mixture for subsequent LC-MS/MS analysis. However, with the
418 use of other techniques, such as desorption electrospray ionization (DESI), which represents a
419 direct-to-MS approach (Deng et al. 2014), much smaller areas of the SPME matrix may be
420 analyzed at a time allowing for laminar or near-laminar resolution. Direct coupling of SPME fibres
421 to MS is the preferred mode, as it provides the most rapid analysis thus preventing diffusion of
422 compounds within the coating and smearing the imprinted layer information. If diffusion of
423 molecules within the fibre is high, it can be prevented by, for example, the inclusion of a divider
424 between two halves of the coating. This would allow the simultaneous measurement of separated
425 compartments of a cortical column. The absolute spatial resolution of SPME is difficult to estimate
426 as SPME operates through diffusion and dynamic equilibration similar to MD. As a consequence,
427 the sampled volume will depend on sampling time, the compound's diffusion coefficient, as well
428 as the target tissue and its properties affecting the rate of diffusion such as tortuosity (Syková
429 2004).

430 *Temporal Resolution.* Several factors determine the appropriate extraction time using
431 SPME. Depending on the goals of an experimenter, resolutions below 5 minutes may be achieved
432 as the detection limit is reached within the first few minutes for most compounds tested (**Fig 1D-**
433 **E**). As sampling continues, the SPME coating will eventually reach an equilibrium point with the
434 external environment (**Fig 1D-E**). In principle, sampling times beyond a stable equilibrium point

435 will result in the same extracted values of compounds. However, in the brain there is no single
436 stable equilibrium point and thus, even with long sampling times, there will be some variation in
437 extracted concentrations. Within the dynamic regime, we can still calculate environmental
438 concentrations from which sampling occurred given knowledge of the extraction time and the
439 dynamic range. The lower limit of this dynamic range that can be informative is determined by the
440 coating's physicochemical characteristics and sample's properties and in practice also volume of
441 desorption and sensitivity of the MS. The analytical technique's sensitivity also practically
442 determines the thickness of the SPME coating as thinner coatings could in principle increase
443 temporal resolution but would extract less compounds overall requiring higher sensitivity to detect.
444 With higher sensitivity, less time is required for the thin coating to extract sufficient amounts to
445 exceed limits of detection and quantitation. This then means that the compound with regards to
446 which the sensitivity is the lowest, limits the temporal resolution because it will have the slowest-
447 to-reach detectable concentration. But as long as the detection threshold is exceeded, the extraction
448 time profiles allow for the calculation of the equilibrium concentration even with pre-equilibrium
449 sampling. However, making measurements in the dynamic range requires consistency of extraction
450 times as differences in time will lead to variations of extraction yields in a range that can be
451 estimated from the SPME extraction time profiles (**Fig 1D-E**). Given the dynamic nature of brain
452 networks and the lack of a stable equilibrium point, we expect consistency in brain states to be one
453 of the biggest factors in reducing replicated variability. Moreover, SPME measurements are
454 inherently an average of the temporal dynamics of the target tissue milieu. This means that due to
455 the bi-directional exchange of neuromodulators from the extracellular space and the SPME
456 coating, longer periods of stable concentration gradients will be more strongly reflected in the
457 extracted measurements.

458 *Utility and Ease of Use.* SPME based microprobe extraction allows for multiple
459 simultaneous measurements that can be reliably repeated within the same measurement sessions
460 at the same locations with no evidence of damage induced disruption of the neurochemical
461 environment. Another critical advantage of SPME over comparable MS-analysis based methods
462 such as MD is its ease of use and accessibility. Due to their similar size to recording
463 microelectrodes used for electrophysiology, little adjustment is required for conducting SPME
464 measurements using existing acute microelectrode positioning systems. Measurements in deeper
465 structures should use an accompanying guide tube (**Fig 1C**) as travelling through non-target tissue
466 will result in unwanted chemical collection. Beyond the collection, a chemistry core could apply
467 LC-MS/MS to the probes allowing for relatively easy quantitation of extracellular compounds of
468 interest.

469 *Detection Methods.* SPME is ultimately a sampling method, much like MD, that provides
470 data for analytical tools such as chromatography and mass spectrometry. In fact, once SPME
471 analytes have been desorbed from the probe into a solvent, data provided by SPME and MD are
472 treated very much the same. Thus, the advancement in detection limits and reliability of post-hoc
473 analytical methods utilized by MD also benefit SPME, and vice versa. However, SPME sample
474 analysis is more reliably and conveniently coupled to LC-MS/MS as it lacks issues such as high
475 salt content of collected dialysate that MD suffers from (Guihen and Connor 2009).

476 *Extension of SPME measurements beyond classical neuromodulators*. A unique advantage
477 of SPME over alternative methods of in vivo detection of compounds within the brain is its
478 potential affinity for hydrophobic compounds. Although MD is capable of collecting
479 metabolomics data similarly to SPME (Anderzhanova and Wotjak 2013; Li et al. 2012; Zhang et
480 al. 2007b), the artificial cerebra-spinal fluid that is commonly traversing the semi-permeable

481 membrane better facilitates the collection of hydrophilic molecules. This means that molecules
482 that cross the semi-permeable membrane and are therefore collected and quantified through LC-
483 MS are much more likely to be hydrophilic. SPME, in contrast, provides balanced analyte
484 coverage, which means that in principle certain SPME matrix coatings have similar affinity for
485 both hydrophilic or hydrophobic compounds (Reyes-garcés et al. 2018). Data collected here
486 includes other neurochemicals of interest such as amino acids (e.g. glutamine, taurine,
487 phenylalanine, etc) that we reliably detected but do not discuss here. In practice, the detection of
488 very polar molecules such as monoamines and catecholamines requires coating chemistry that
489 facilitates hydrophilic compound extraction. Comparatively many lipids play important roles in
490 intracellular signaling and have been suggested to provide biomarkers for psychiatric disorders
491 (Tamiji and Crawford 2011; Yehuda et al. 1999), therefore making SPME a potentially versatile
492 and comprehensive tool for brain neurochemistry studies.
493
494 **Future direction and improvements to the SPME neurochemical sensing.** The next immediate
495 steps for the continued testing of SPME's utility as a neurochemical sampling method is to evaluate
496 its ability to report behavioral state dependent changes in extracellular neuromodulator
497 concentrations. Similar testing as described here will be conducted with varying, stable behavioral
498 states such as passive engagement, active task engagement, and drowsy/sleepiness. We predict
499 that the various brain regions tested will display different changes in neuromodulator
500 concentrations as a function of behavioral state.
501 Several improvements to the protocol can be made in order to make SPME more
502 informative. Using a more sensitive MS would reduce detection thresholds and increase sensitivity
503 in detecting compounds not successfully measured here such as GABA, serotonin or

504 norepinephrine. This would be very impactful, especially in the case of serotonin for reasons
505 discussed above. Additionally, efforts could be made to improve the extracting phase synthesis
506 and functionalization protocols and increase the extracting capabilities of SPME probes.
507 Moreover, in order to decrease the MS background and interferences in the range of small
508 molecules, derivatization strategy could be considered.

509 For GABA, the most promising strategy is post-desorption derivatization by reagent
510 increasing the compound's hydrophobicity resulting in better MS signal such as benzoyl chloride
511 (Wong 2016). Catecholamine and acetylcholine detection may be improved by optimizing the
512 post-sampling analysis pipeline. Improvements can be made at several steps in order to better
513 preserve and quantify catecholamines: (1) faster coupling of sampling to desorption (2) trying
514 various antioxidant solutions and other preservatives for maintaining catecholamine integrity and
515 (3) faster analysis of the desorbed analytes. Faster coupling of sampling to desorption could be
516 achieved through a more stream-lined process of fibre placement and retraction involving a static
517 cannula maintained through several sampling events. This mechanism would also allow for a faster
518 replacement of SPME probes resulting in a shorter delay between consecutive measurements.

519 A preliminary experiment using both spiked artificial cerebra-spinal fluid (aCSF) and lamb
520 brain homogenate with very high, known concentrations of all target compounds yielded
521 detectable concentrations of all target compounds indicating that the extracting phase of the SPME
522 probe is capable of capturing all compounds of interest. Furthermore, simultaneously collected
523 replicates displayed very little loss of collected compounds over several days within a -80°C
524 freezer (data not shown). Various strategies were compared for storage and placement of extraction
525 fibres in desorption solvent prior to -80°C storage seemed most reliable for many compounds and
526 will be the storage method utilized in the future. Such findings neither support nor antagonize the

527 suggested strategies for improving SPME yield and sensitivity in primates as detection properties
528 within the aCSF and lamb brain homogenate may not accurately reflect those observed in vivo in
529 primates. This is likely contributed to by the dynamic and highly regulated nature of target
530 compounds within the extracellular space of the brain and the dynamic equilibrium between the
531 extracting phase of the SPME probes and the extracellular environment. Further tests of the
532 possible differences between these mediums and improvement strategies to SPME probes are
533 subject for future studies.
534
535 **Implications for Understanding and Treating Psychiatric Disease States.** Most psychiatric
536 disorders are accompanied by neuromodulatory dysregulation (Millan et al. 2012). However, this
537 fact is seldom studied in a multi-modulatory manner with a single or few nuclei or neurochemicals
538 being observed at a time. This is an increasingly evident problem because models attributing
539 symptoms of a disorder to a single neuromodulator often fall short in explaining many symptoms
540 (Bohnen et al. 2015; Remy et al. 2005). For example, in Parkinson's disease, outside of the well
541 characterized dopaminergic deficits, there is evidence for deficits in noradrenergic, cholinergic
542 and serotonergic systems as well (Halliday et al. 1990, 2014; Moehle et al. 2017). Many cognitive
543 deficits observed within Parkinson's disease are linked to such non-dopaminergic deficits. Such
544 findings emphasize the need to simultaneously observe multiple neuromodulatory systems. Thus
545 the simultaneous measurement of multiple neuromodulators, in multiple brain regions within
546 healthy and clinical populations will allow for a better understanding of the underlying causes of
547 symptoms and progression of psychiatric disorders (Anderzhanova and Wotjak 2015; Avery and
548 Krichmar 2017; Millan et al. 2012).

549 A better understanding of psychiatric disorders through multi-modulator methods may also
550 lead to more accurate understanding of the action of pharmacological agents. Previously, many
551 studies aimed at identifying the locus of action of a pharmacological agent have used local
552 injection methods such as iontophoresis or microinjections (Lapiz and Morilak 2006; Wang et al.
553 2007). Although highly informative about the role of neuromodulators in modulating the activity
554 of individual cells and circuits, this approach does not allow physiologically realistic exploration
555 of a systemically administered pharmacological agent. Pharmacological agents are often
556 administered in some systemic fashion and even with highly specific receptor affinities, may
557 interact with multiple neuromodulatory systems through the actions of heteroreceptors (Avery and
558 Krichmar 2017; Gobert et al. 1998; Millan et al. 2015). Multi-modulator measurements, as
559 described here, will allow for a better understanding of pharmacological agents, as well as provide
560 novel insights into the development of more effective drugs or combinations of drugs to better
561 treat the clinical population.
562
563 **Conclusion**. We described a novel SPME protocol capable of simultaneous, multi-modulator
564 measurements of multiple brain regions. Our results suggest that SPME both supplements current
565 methods of neuromodulator detection and allows for novel measurements previously not possible
566 for the investigation and dissection of neuromodulatory systems, their role in physiological brain
567 processes and their modulation by pharmacological agents.
568
569 **Acknowledgments**
570 This research was supported by grants from the Canadian Institutes of Health Research (CIHR),
571 the Natural Sciences and Engineering Research Council of Canada (NSERC) and the Ontario

572 Ministry of Economic Development and Innovation (MEDI). We thank Dr. Hongying Wang for
573 invaluable help with animal care. We thank Thermo Scientifc for providing the triple quadrupole
574 mass spectrometer TSQ Quantiva used in this work as a loan to our laboratory. The authors
575 thankfully acknowledge Pfizer Canada Inc., Merck Canada Inc., Quebec Consortium for Drug
576 Discovery (CQDM), Brain Canada, and Ontario Brain Institute for the grant "Solid phase
577 microextraction-based integrated platform for untargeted and targeted in vivo brain studies".

578

579 **Conflicts of interest**

580 None of the authors have any conflict to disclose.

581 **References**
582
583 **Alam N**, **Pawliszyn J**. Numerical Simulation and Experimental Validation of Calibrant-Loaded
584 Extraction Phase Standardization Approach. *Anal Chem* 88: 8632–8639, 2016.
585 **Anderzhanova E**, **Wotjak CT**. Brain microdialysis and its applications in experimental
586 neurochemistry. *Cell Tissue Res* 354: 27–39, 2013.
587 **Anderzhanova E**, **Wotjak CT**. NextGen Brain Microdialysis : Applying Modern Metabolomics
588 Technology to the Analysis of Extracellular Fluid in the Central Nervous System. *Mol*
589 *Neuropsychiatry* 1: 60–67, 2015.
590 **Arnsten AFT**, **Paspalas CD**, **Gamo NJ**, **Yang Y**, **Wang M**. Dynamic network connectivity: A
591 new form of neuroplasticity. *Trends Cogn Sci* 14: 365–375, 2010.
592 **Ascenzo MD**, **Fellin T**, **Terunuma M**, **Revilla-sanchez R**, **Meaney DF**, **Auberson YP**, **Moss**
593 **SJ**, **Haydon PG**. mGluR5 stimulates gliotransmission in the nucleus accumbens. *Proc Natl Acad*
594 *Sci* 104: 1995–2000, 2006.
595 **Avery MC**, **Krichmar JL**. Neuromodulatory Systems and Their Interactions : A Review of
596 Models , Theories , and Experiments. *Front Neural Circuits* 11: 1–18, 2017.
597 **Bohnen NB**, **Albin R**, **Muller MLTM**, **Petrou M**, **Kotagal V**, **Koeppe RA**, **Scott PJH**, **Frey**
598 **KA**. Frequency of Cholinergic and Caudate Nucleus Dopaminergic Deficits Across the
599 Predemented Cognitive Spectrum of Parkinson Disease and Evidence of Interaction Effects.
600 *JAMA Neurol* 72: 194–200, 2015.
601 **Buck K**, **Voehringer P**, **Ferger B**. Rapid analysis of GABA and glutamate in microdialysis
602 samples using high performance liquid chromatography and tandem mass spectrometry. *J*
603 *Neurosci Methods* 182: 78–84, 2009.
604 **Cudjoe E**, **Bojko B**, **de Lannoy I**, **Saldivia V**, **Pawliszyn J**. Solid-Phase Microextraction: A
605 Complementary In Vivo Sampling Method to Microdialysis. *Angew Chemie Int Ed* 52: 12124–
606 12126, 2013.
607 **Cudjoe E**, **Pawliszyn J**. Optimization of solid phase microextraction coatings for liquid
608 chromatography mass spectrometry determination of neurotransmitters. *J Chromatogr A* 1341:
609 1–7, 2014.
610 **Dale N**, **Hatz S**, **Tian F**, **Llaudet E**. Listening to the brain: Microelectrode biosensors for
611 neurochemicals. *Trends Biotechnol* 23: 420–428, 2005.
612 **Deng J**, **Yang Y**, **Wang X**, **Luan T**. Strategies for coupling solid-phase microextraction with
613 mass spectrometry. *TrAC - Trends Anal Chem* 55: 55–67, 2014.
614 **Disney AA**, **McKinney C**, **Grissom L**, **Lu X**, **Reynolds JH**. A multi-site array for combined
615 local electrochemistry and electrophysiology in the non-human primate brain. *J Neurosci*
616 *Methods* 255: 29–37, 2015.
617 **Fisher RE**, **Morris ED**, **Alpert NM**, **Fischman AJ**. In Vivo Imaging of Neuromodulatory
618 Synaptic Transmission Using PET : A Review of Relevant Neurophysiology. *Hum Brain Mapp*
619 3: 24–34, 1995.
620 **Ghersi C**, **Bonfanti A**, **Manzari B**, **Feligioni M**, **Raiteri M**, **Pittaluga A**. Pharmacological
621 heterogeneity of release-regulating presynaptic AMPA / kainate receptors in the rat brain : study
622 with receptor antagonists. *Neurochem Int* 42: 283–292, 2003.
623 **Gobert A**, **Audinot V**, **Cistarelli L**, **Millan MJ**. Simultaneous quantification of serotonin,
624 dopamine and noradrenaline levels in single frontal cortex dialysates of freely-moving rats
625 reaveals a complex pattern of reciprocal auto- and heteroreceptor-mediated control of release.
626 *Neuroscience* 84: 413–429, 1998.

Goldman-Rakic PS, **Lidow MS**, **Gallager DW**. Overlap of dopaminergic, adrenergic, and serotoninergic receptors and complementarity of their subtypes in primate prefrontal cortex. *J Neurosci* 10: 2125–2138, 1990.

Gómez-Ríos GA, **Tascon M**, **Reyes-garcés N**, **Boyacı E**. Quantitative analysis of biofluid spots by coated blade spray mass spectrometry , a new approach to rapid screening. *Sci Rep* 7: 1–7, 2017.

Granger AJ, **Mulder N**, **Saunders A**, **Sabatini BL**. Cotransmission of acetylcholine and GABA. *Neuropharmacology* 100: 40–46, 2016.

Grilli M, **Zappettini S**, **Zanardi A**, **Lagomarsino F**, **Pittaluga A**, **Zoli M**, **Marchi M**. Exposure to an enriched environment selectively increases the functional response of the pre-synaptic NMDA receptors which modulate noradrenaline release in mouse hippocampus. *J Neurochem* 110: 1598–1606, 2009.

Guihen E, **Connor WTO**. Current separation and detection methods in microdialysis the drive towards sensitivity and speed. *Electrophoresis* 30: 2062–2075, 2009.

Haber SN, **Knutson B**. The reward circuit: Linking primate anatomy and human imaging. *Neuropsychopharmacology* 35: 4–26, 2010.

Halliday GM, **Leverenz JB**, **Schneider JS**, **Adler CH**. The Neurobiological Basis of Cognitive Impairment in Parkinson's Disease. *Mov Disord* 29: 634–650, 2014.

Halliday GM, **Li YW**, **Blumbergs PC**, **Joh TH**, **Cotton PRGH**, **Howe PRC**, **Blessing WW**, **Geffen LB**. Neuropathology of Immunohstochemically Idendied Brainstem Neurons in Parkinson's Disease. *Am Neurol Assoc* 27: 373–385, 1990.

Hassan SF, **Zumut S**, **Burke PG**, **Mcmullan S**, **Cornish JL**, **Goodchild AK**. Comparison of noradrenlaine, dopamine and serotonin in mediating the tachycardic and thermogenic effects of methamphetamine in the ventral medial prefrontal cortex. *Neuroscience* 295: 209–220, 2015.

Hassani SA, **Oemisch M**, **Balcarras M**, **Westendorff S**, **Ardid S**, **van der Meer MA**, **Tiesinga P**, **Womelsdorf T**. A computational psychiatry approach identifies how alpha-2A noradrenergic agonist Guanfacine affects feature-based reinforcement learning in the macaque. *Sci Rep* 7: 40606, 2017.

Holloway ZR, **Freels TG**, **Comstock JF**, **Nolen HG**, **Sable HJ**, **Lester DB**. Comparing phasic dopamine dynamics in the striatum, nucleus accumbens, amygdala, and medial prefrontal cortex. *Synapse* 73: 1–15, 2019.

Howe WM, **Gritton HJ**, **Lusk NA**, **Roberts EA**, **Hetrick VL**, **Berke JD**, **Sarter M**. Acetylcholine Release in Prefrontal Cortex Promotes Gamma Oscillations and Theta–Gamma Coupling during Cue Detection. *J Neurosci* 37: 3215–3230, 2017.

Jacobs CB, **Peairs MJ**, **Venton BJ**. Review: Carbon nanotube based electrochemical sensors for biomolecules. *Anal Chim Acta* 662: 105–127, 2010.

Kennedy RT. Emerging trends in in vivo neurochemical monitoring by microdialysis. *Curr Opin Chem Biol* 17: 860–867, 2013.

Kodama T, **Hikosaka K**, **Honda Y**, **Kojima T**, **Tsutsui K**, **Watanabe M**. Dopamine and glutamate release in the anterior default system during rest : A monkey microdialysis study. *Behav Brain Res* 294: 194–197, 2015.

Kodama T, **Hikosaka K**, **Watanabe M**. Differential changes in glutamate concentration in the primate prefrontal cortex during spatial delayed alternation and sensory-guided tasks. *Exp Brain Res* 145: 133–141, 2002.

Kodama T, **Kojima T**, **Honda Y**, **Hosokawa T**, **Tsutsui K**, **Watanabe M**. Oral Administration of Methylphenidate (Ritalin) Affects Dopamine Release Differentially Between the Prefrontal

673 Cortex and Striatum: A Microdialysis Study in the Monkey. *J Neurosci* 37: 2387–2394, 2017.
674 **König M**, **Thinnes A**, **Klein J**. Microdialysis and its use in behavioural studies: Focus on
675 acetylcholine. *J Neurosci Methods* 300: 206–215, 2018.
676 **Kreitzer AC**. Physiology and pharmacology of striatal neurons. *Annu Rev Neurosci* 32: 127–47,
677 2009.
678 **Lapiz MDS**, **Morilak DA**. Noradrenergic modulation of cognitive function in rat medial
679 prefrontal cortex as measured by attentional set shifting capability. *Neuroscience* 137: 1039–
680 1049, 2006.
681 **Lendor S**, **Hassani S-A**, **Boyaci E**, **Singh V**, **Womelsdorf T**, **Pawliszyn J**. Solid Phase
682 Microextraction-Based Miniaturized Probe and Protocol for Extraction of Neurotransmitters
683 from Brains in Vivo. *Anal Chem* 91: 4896–4905, 2019.
684 **Li J**, **von Pföstl V**, **Zaldivar D**, **Zhang X**, **Logothetis NK**, **Rauch A**. Measuring multiple
685 neurochemicals and related metabolites in blood and brain of the rhesus monkey by using dual
686 microdialysis sampling and capillary hydrophilic interaction chromatography-mass spectrometry.
687 *Anal Bioanal Chem* 402: 2545–2554, 2012.
688 **Luccini E**, **Musante V**, **Neri E**, **Brambilla Bas M**, **Severi P**, **Raiteri M**, **Pittaluga A**.
689 Functional interactions between presynaptic NMDA receptors and metabotropic glutamate
690 receptors co-expressed on rat and human noradrenergic terminals. *Br J Pharmacol* 151: 1087–
691 1094, 2007.
692 **Marder E**. Overview Neuromodulation of Neuronal Circuits: Back to the Future. *Neuron* 76: 1–
693 11, 2012.
694 **Marder E**, **O'Leary T**, **Shruti S**. Neuromodulation of Circuits with Variable Parameters: Single
695 Neurons and Small Circuits Reveal Principles of State-Dependent and Robust Neuromodulation.
696 *Annu Rev Neurosci* 37: 329–346, 2014.
697 **McGinley MJ**, **Vinck M**, **Reimer J**, **Batista-Brito R**, **Zagha E**, **Cadwell CR**, **Tolias AS**,
698 **Cardin JA**, **McCormick DA**. Waking State: Rapid Variations Modulate Neural and Behavioral
699 Responses. *Neuron* 87: 1143–1161, 2015.
700 **Millan MJ**, **Agid Y**, **Brüne M**, **Bullmore ET**, **Carter CS**, **Clayton NS**, **Connor R**, **Davis S**,
701 **Deakin B**, **DeRubeis RJ**, **Dubois B**, **Geyer MA**, **Goodwin GM**, **Gorwood P**, **Jay TM**, **Joëls**
702 **M**, **Mansuy IM**, **Meyer-Lindenberg A**, **Murphy D**, **Rolls E**, **Saletu B**, **Spedding M**, **Sweeney**
703 **J**, **Whittington M**, **Young LJ**. Cognitive dysfunction in psychiatric disorders: characteristics,
704 causes and the quest for improved therapy. *Nat Rev Drug Discov* 11: 141–168, 2012.
705 **Millan MJ**, **Goodwin GM**, **Meyer-lindenberg A**, **Ove S**. Learning from the past and looking to
706 the future : Emerging perspectives for improving the treatment of psychiatric disorders. *Eur*
707 *Neuropsychopharmacol* 25: 599–656, 2015.
708 **Moehle MS**, **Pancani T**, **Byun N**, **Yohn SE**, **Wilson GH**, **Dickerson JW**, **Remke DH**, **Xiang**
709 **Z**, **Niswender CM**, **Wess J**, **Jones CK**, **Lindsley CW**, **Rook JM**, **Conn PJ**. Cholinergic
710 Projections to the Substantia Nigra Pars Reticulata Inhibit Dopamine Modulation of Basal
711 Ganglia through the M4Muscarinic Receptor. *Neuron* 96: 1358–1372, 2017.
712 **Moghaddam B**. Stress Preferentially Increases Extraneurona Levels of Excitatory Amino Acids
713 in the Prefrontal Cortex : Comparison to Hippocampus and Basal Ganglia. *J Neurochem* 60:
714 1650–1657, 1993.
715 **Moussawi K**, **Riegel A**, **Nair S**, **Kalivas PW**, **Bargas J**, **Nacional U**. Extracellular glutamate :
716 functional compartments operate in different concentration ranges. *Front Syst Neurosci* 5: 1–9,
717 2011.
718 **Oemisch M**, **Westendorff S**, **Oemisch M**, **Westendorff S**, **Everling S**, **Womelsdorf XT**.

Interareal Spike-Train Correlations of Anterior Cingulate and Dorsal Prefrontal Cortex during Attention Shifts Interareal Spike-Train Correlations of Anterior Cingulate and Dorsal Prefrontal Cortex during Attention Shifts. *J Neurosci* 35: 13076–13089, 2015.

Ouyang G, **Pawliszyn J**. Configurations and calibration methods for passive sampling techniques. *J Chromatogr A* 1168: 226–235, 2007.

Parikh V, **Kozak R**, **Martinez V**, **Sarter M**. Prefrontal Acetylcholine Release Controls Cue Detection on Multiple Timescales. *Neuron* 56: 141–154, 2007.

Pawliszyn J. Theory of Solid-Phase Microextraction. *J Chromatogr Sci* 38: 270–278, 2000.

Pawliszyn J. Theory of Solid-Phase Microextraction. In: *Handbook of Solid Phase Microextraction*, edited by Pawliszyn J. Elsevier, 2012, p. 13–59.

Paxinos G, **Huang X**, **Toga A**. *The Rhesus Monkey Brain in Stereotaxic Coordinates*. 2000.

Perry M, **Li Q**, **Kennedy RT**. Review of recent advances in analytical techniques for the determination of neurotransmitters. *Anal Chim Acta* 653: 1–22, 2009.

Pittaluga A. Presynaptic release-regulating mGlu1 receptors in central nervous system. *Front Pharmacol* 7: 1–15, 2016.

Pittaluga A, **Feligioni M**, **Longordo F**, **Luccini E**, **Raiteri M**. Trafficking of presynaptic AMPA receptors mediating neurotransmitter release : Neuronal selectivity and relationships with sensitivity to cyclothiazide. *Neuropharmacology* 50: 286–296, 2006.

Quintero JE, **Day BK**, **Zhang Z**, **Grondin R**, **Stephens ML**, **Huettl P**, **Pomerleau F**, **Gash DM**, **Gerhardt GA**. Amperometric measures of age-related changes in glutamate regulation in the cortex of rhesus monkeys. *Exp Neurol* 208: 238–246, 2007.

Reimer J, **Froudarakis E**, **Cadwell CR**, **Yatsenko D**, **Denfield GH**, **Tolias AS**. Pupil Fluctuations Track Fast Switching of Cortical States during Quiet Wakefulness. *Neuron* 84: 355–362, 2014.

Reimer J, **McGinley MJ**, **Liu Y**, **Rodenkirch C**, **Wang Q**, **McCormick DA**, **Tolias AS**. Pupil fluctuations track rapid changes in adrenergic and cholinergic activity in cortex. *Nat Commun* 7: 1–7, 2016.

Remy P, **Doder M**, **Lees A**, **Turjanski N**, **Brooks D**. Depression in Parkinson ' s disease: loss of dopamine and noradrenaline innervation in the limbic system. *Brain* 128: 1314–1322, 2005.

Reyes-garcés N, **Gionfriddo E**, **Gómez-Ríos GA**, **Alam MN**, **Boyaci E**, **Bojko B**, **Singh V**, **Grandy J**, **Pawliszyn J**. Advances in Solid Phase Microextraction and Perspective on Future Directions. *Anal Chem* 90: 302–360, 2018.

Santana N, **Mengod G**, **Artigas F**. Expression of a1-adrenergic receptors in rat prefrontal cortex: cellular co-localization with 5-HT2A receptors. *Int J Neuropsychopharmacol* 16: 1139–1151, 2018.

Santello M, **Calì C**, **Bezzi P**. Gliotransmission and the Tripartite Synapse. In: *Synaptic Plasticity. Advances in Experimental Medicine and Biology*, edited by Kreutz M, Sala C. 2012, p. 307–331.

Schluter EW, **Mitz AR**, **Cheer JF**, **Averbeck BB**. Real-time dopamine measurement in awake monkeys. *PLoS One* 9, 2014.

Schwartz J, **Javitch J**. Neurotransmitters. In: *Principles of Neural Science*, edited by Kandel E, Schwartz J, Jessell T, Siegelbaum S, Hudspeth A. 2013, p. 289–306.

Schwerdt HN, **Shimazu H**, **Amemori K**, **Amemori S**, **Tierney PL**, **Gibson DJ**, **Hong S**, **Yoshida T**, **Langer R**, **Cima MJ**, **Graybiel AM**. Long-term dopamine neurochemical monitoring in primates. *Proc Natl Acad Sci* 114: 13260–13265, 2017.

Syková E. Extrasynaptic volume transmission and diffusion parameters of the extracellular

space. *Neuroscience* 129: 861–876, 2004.
Tamiji J, **Crawford A**. The Neurobiology of Lipid Metabolism in. *Eur PMC* 18: 98–112, 2011.
Thiele A, **Bellgrove MA**. Neuromodulation of Attention. *Neuron* 97: 769–785, 2018.
Vartak D, **Togt C Van Der**, **Vugt B Van**, **Roelfsema PR**. Electrochemical measurement of acetylcholine in the dorsolateral prefrontal cortex : A technical report. *BioRXiv* 1–25, 2017.
Vijayraghavan S, **Wang M**, **Birnbaum SG**, **Williams G V.**, **Arnsten AFT**. Inverted-U dopamine D1 receptor actions on prefrontal neurons engaged in working memory. *Nat Neurosci* 10: 376–384, 2007.
Vizi ES. Role of high-affinity receptors and membrane transporters in nonsynaptic communication and drug action in the central nervous system. *Pharmacol Rev* 52: 63–89, 2000.
Wang JKT, **Andrews H**, **Thukral V**. Presynaptic Glutamate Receptors Regulate Noradrenaline Release from Isolated Nerve Terminals. *J Neurochem* 58: 204–211, 1992.
Wang M, **Ramos BP**, **Paspalas CD**, **Shu Y**, **Simen A**, **Duque A**, **Vijayraghavan S**, **Brennan A**, **Dudley A**, **Nou E**, **Mazer J a.**, **McCormick D a.**, **Arnsten a. FT**. alpha2A-Adrenoceptors Strengthen Working Memory Networks by Inhibiting cAMP-HCN Channel Signaling in Prefrontal Cortex. *Cell* 129: 397–410, 2007.
Watanabe M, **Kodama T**, **Hikosaka K**. Increase of Extracellular Dopamine in Primate Prefrontal Cortex During a Working Memory Task. *J Neurophysiol* 78: 2795–2798, 1997.
Watson CJ, **Venton BJ**, **Kennedy RT**. In Vivo Measurements of Neurotransmitters by Microdialysis Sampling. *Anal Chem* 78: 1391–1399, 2006.
Yehuda S, **Rabinovitz S**, **Mostofsky DI**. Mini-Review Essential Fatty Acids Are Mediators of Brain Biochemistry and Cognitive Functions. *J Neurosci Res* 56: 565–570, 1999.
Yoshimi K, **Kumada S**, **Weitemier A**, **Jo T**, **Inoue M**. Reward-induced phasic dopamine release in the monkey ventral striatum and putamen. *PLoS One* 10: 1–22, 2015.
Zapata A, **Chefer VI**, **Parrot S**, **Denoroy L**. Detection and Quantification of Neurotransmitters in Dialysates. *Curr Protoc Neurosci* 63: 1–35, 2013.
Zhang X, **Es-haghi A**, **Musteata FM**, **Ouyang G**, **Pawliszyn J**. Quantitative in Vivo Microsampling for Pharmacokinetic Studies Based on an Integrated Solid-Phase Microextraction System. *Anal Chem* 79: 4507–4513, 2007a.
Zhang X, **Rauch A**, **Lee H**, **Xiao H**, **Rainer G**, **Logothetis N**. Capillary hydrophilic interaction chromatography/mass spectrometry for simultaneous determination of multiple neurotransmitters in primate cerebral cortex. *Rapid Commun Mass Spectrom* 21: 3621–3628, 2007b.

798 **Fig 1. SPME sampling procedure, extraction time profiles and measurement locations**.
799 (A) Dimensions of the SPME probe and the accompanying cannula. There was a 3000 µm buffer
800 from the opening of the cannula and the start of the SPME coating. The SPME coating spanned
801 195 µm at the tip. The SPME coating made up the terminal 3000 µm of the entire probe and was
802 placed in a cannula with an internal diameter of 200 µm and an external diameter of 270 µm. (B)
803 Tungsten microelectrodes were lowered into the brain guided by 3 T magnetic resonance (MR)
804 images in order to map the depth at which detectable spiking was observed matching expectations
805 from the MR images. (C) SPME probes and their accompanying cannulas in all brain areas were
806 then simultaneously lowered to 200 µm above the point of first observable firing in the target brain
807 region and the SPME probes were lowered to expose only the 3000 µm SPME coating. After 20
808 minutes of extraction, the SPME probes were then retracted 3000 µm back into the cannula and
809 the probes plus their accompanying cannulas were removed from the brain. The table inset into
810 the figure provides the velocities and times of each probe and cannula as they transitioned between
811 the extraction steps. (D) In vitro extraction quantities of Glutamate in ng and (E) Dopamine in ng
812 over time utilized to select in vivo extraction times. The linear "kinetic" regime and "equilibrium"
813 regime are labelled with the dynamic range being in between. (F**)** Anatomical locations of SPME
814 sampling events in the right hemisphere of two Rhesus Macaques. Target brain regions are
815 highlighted in red and include two cortical regions, prefrontal cortex (PFC) area 8 and premotor
816 cortex (PreM) area 6 as well as a subcortical region: the head of the caudate.
817
818 **Fig 2. Changes in SPME sampling over time.**
819 Changes in the normalized concentrations of the observed neuromodulators across daily sampling
820 sessions in each sampled brain region. The median concentration of (A) Glutamate (B)
821 acetylcholine (C) choline and dopamine (D) with standard error of the median plotted for each
822 sampling time and location. Data was normalization for each subject separately and for the
823 respective neurochemical and area combinations. Sampling locations are represented by different
824 lines: solid line for the prefrontal cortex, dashed line for the premotor cortex and dotted line for
825 the caudate nucleus. Sampling events were 20 minutes in length and the time between the end of
826 one sampling event to the start of the next sampling event was 40 minutes (STD 2 minutes) making
827 the second sampling event 40 minutes and the third 100 minutes from the initial measurement. No
828 significant change was observed for any neuromodulator in any brain region (Wilcoxon rank sum
829 test). Note that a single prefrontal choline data point was excluded in this analysis for being >4
830 standard deviations from the median (data point is present in **Fig 3a**).
831
832 **Fig 3. SPME sampling of the macaque brain.**
833 SPME probes extract from the cortex (PFC and PreM6) as well as the caudate of two adult
834 macaques after 20 minutes of extraction within the respective brain region. Median and standard
835 error of the median of n= 12 probes for animal As and n= 9 probes for animal Ke with no data
836 excluded. Four neuromodulators were reliably measured: glutamate, dopamine, acetylcholine, and
837 choline (orange, green, purple, red respectively). All brain regions had high concentrations of
838 glutamate and relatively much lower concentrations of acetylcholine and choline extracted (with
839 the exception of animal Ke PreM6 lacking detectable acetylcholine). The only tested region to
840 yield measurable dopamine was the caudate. The dashed blue line depicts the limit of detection
841 (LOD).

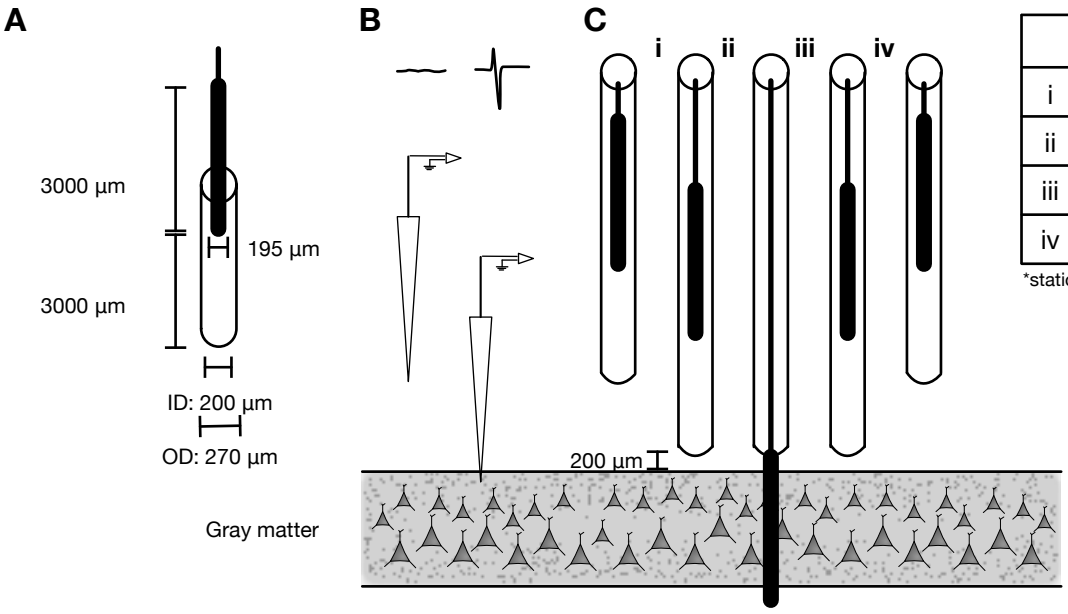

	fibre	cannula	time
i	30 µm/s	30 µm/s	variable
ii	30 µm/s	-	200s
iii	30 µm/s	-	1200s* + 200s
iv	30 µm/s	30 µm/s	variable

*stationary: extraction period of 20 min

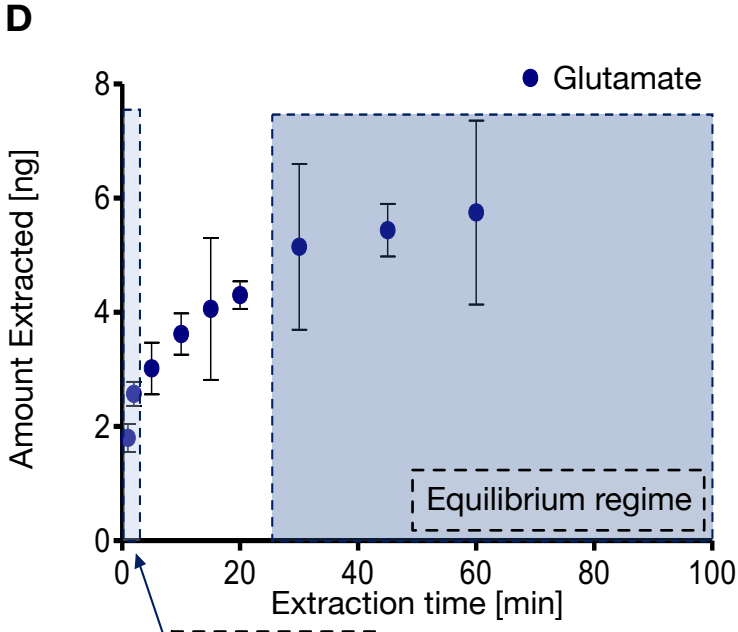

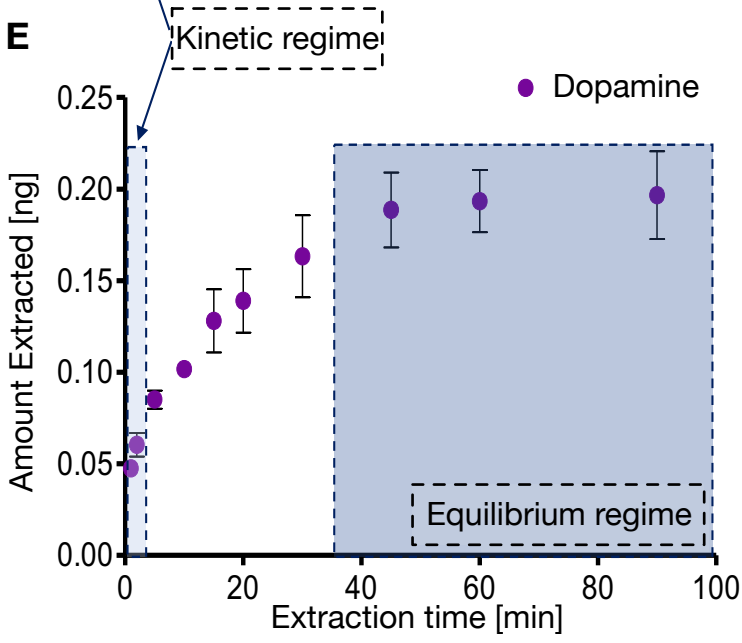

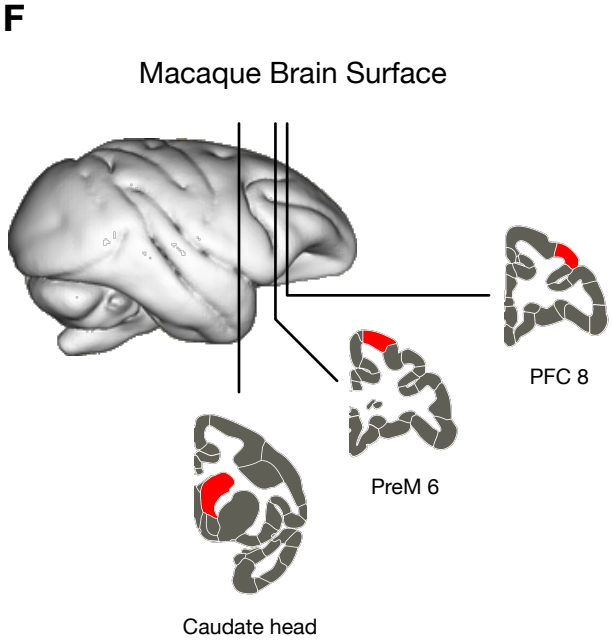

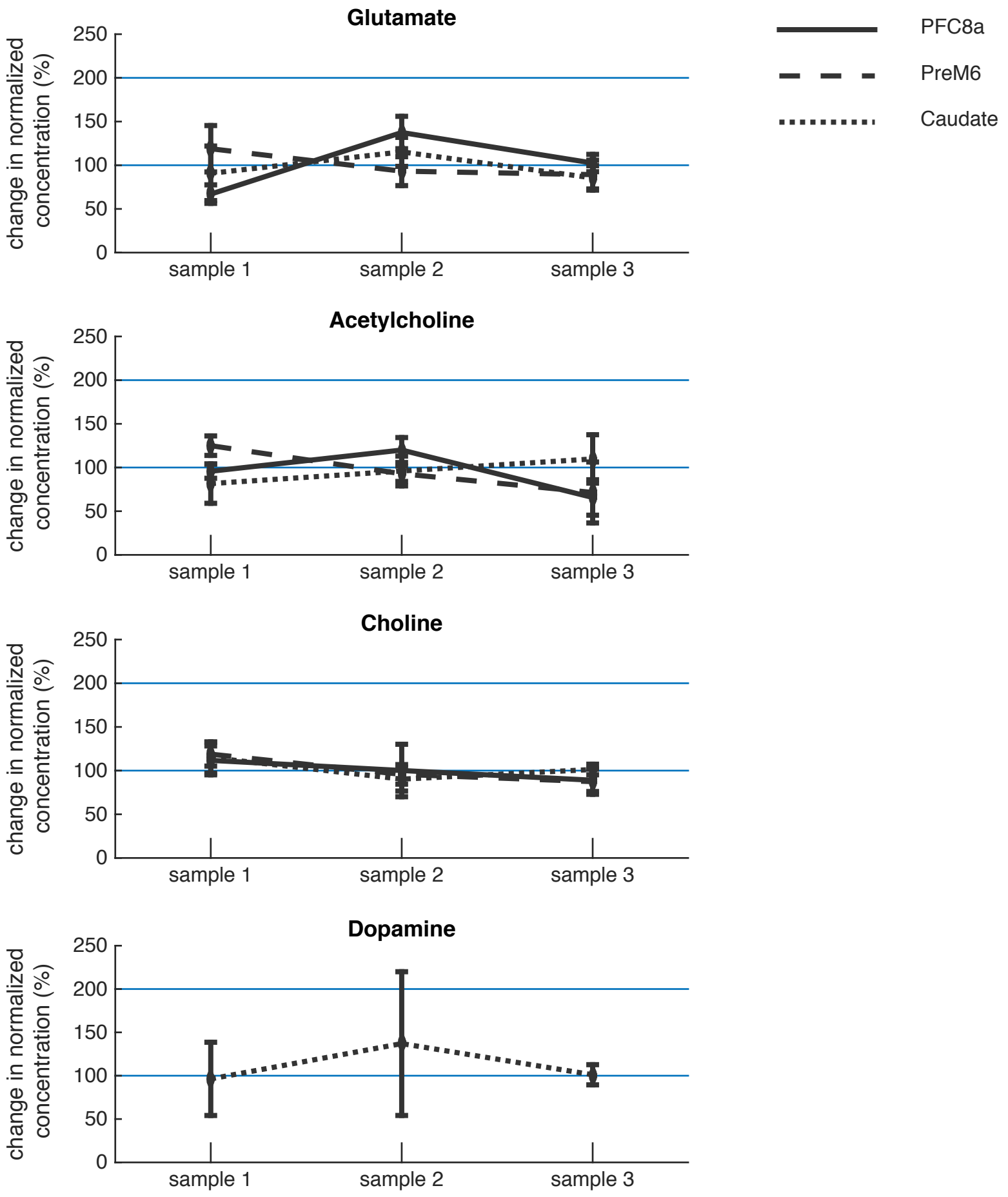
Glutamate
Acetylcholine
Choline
Dopamine
change in normalized concentration (%)
250
200
150
100
50
0
sample 1
sample 2
sample 3
PFC8a
PreM6
Caudate

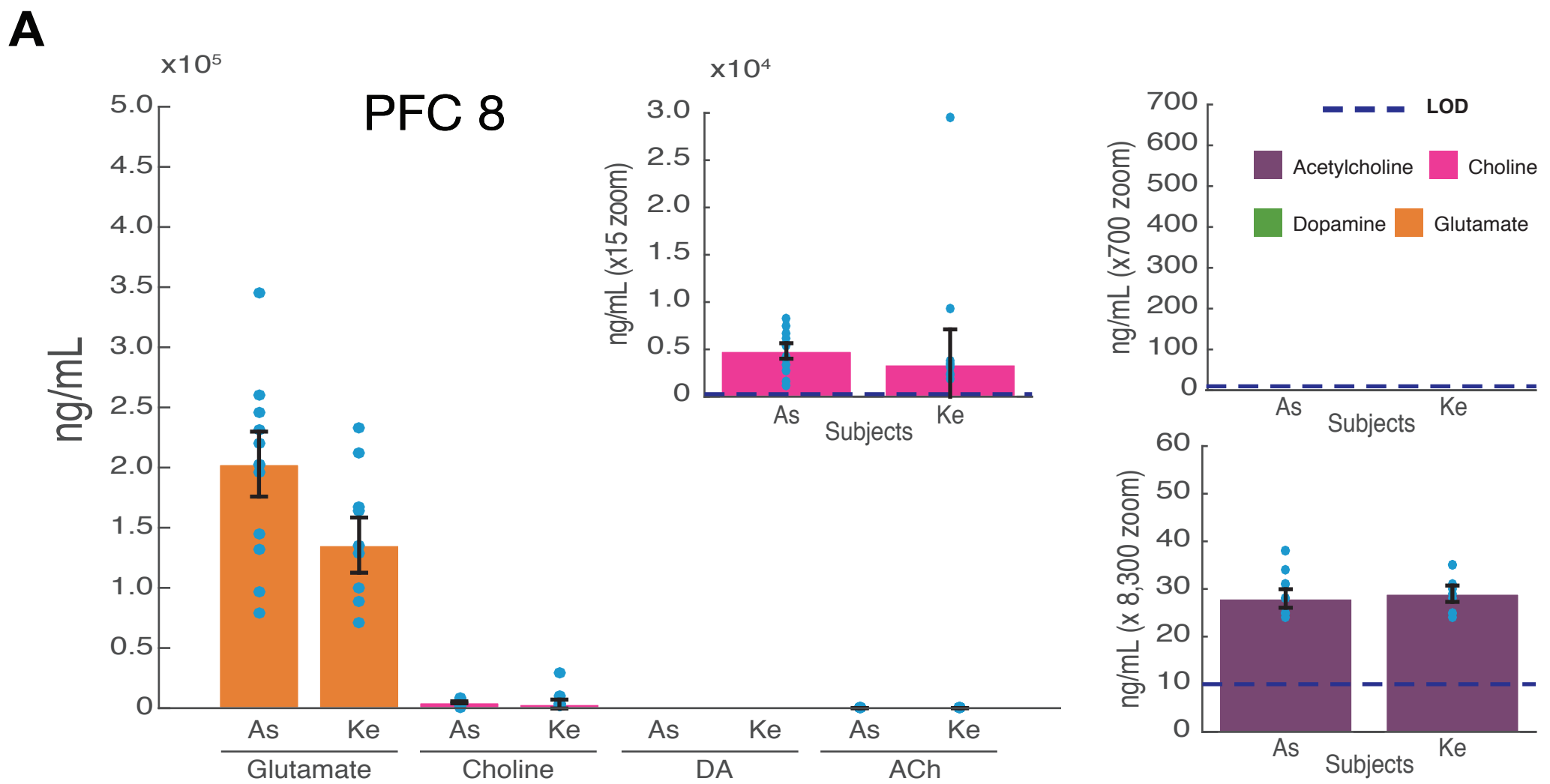
A
PFC 8
x10⁵
ng/mL
5.0
4.5
4.0
3.5
3.0
2.5
2.0
1.5
1.0
0.5
0
As
Ke
Glutamate
Choline
DA
ACh
x10⁴
ng/mL (x15 zoom)
Subjects
LOD
Acetylcholine
Choline
Dopamine
Glutamate
ng/mL (x700 zoom)
ng/mL (x 8,300 zoom)

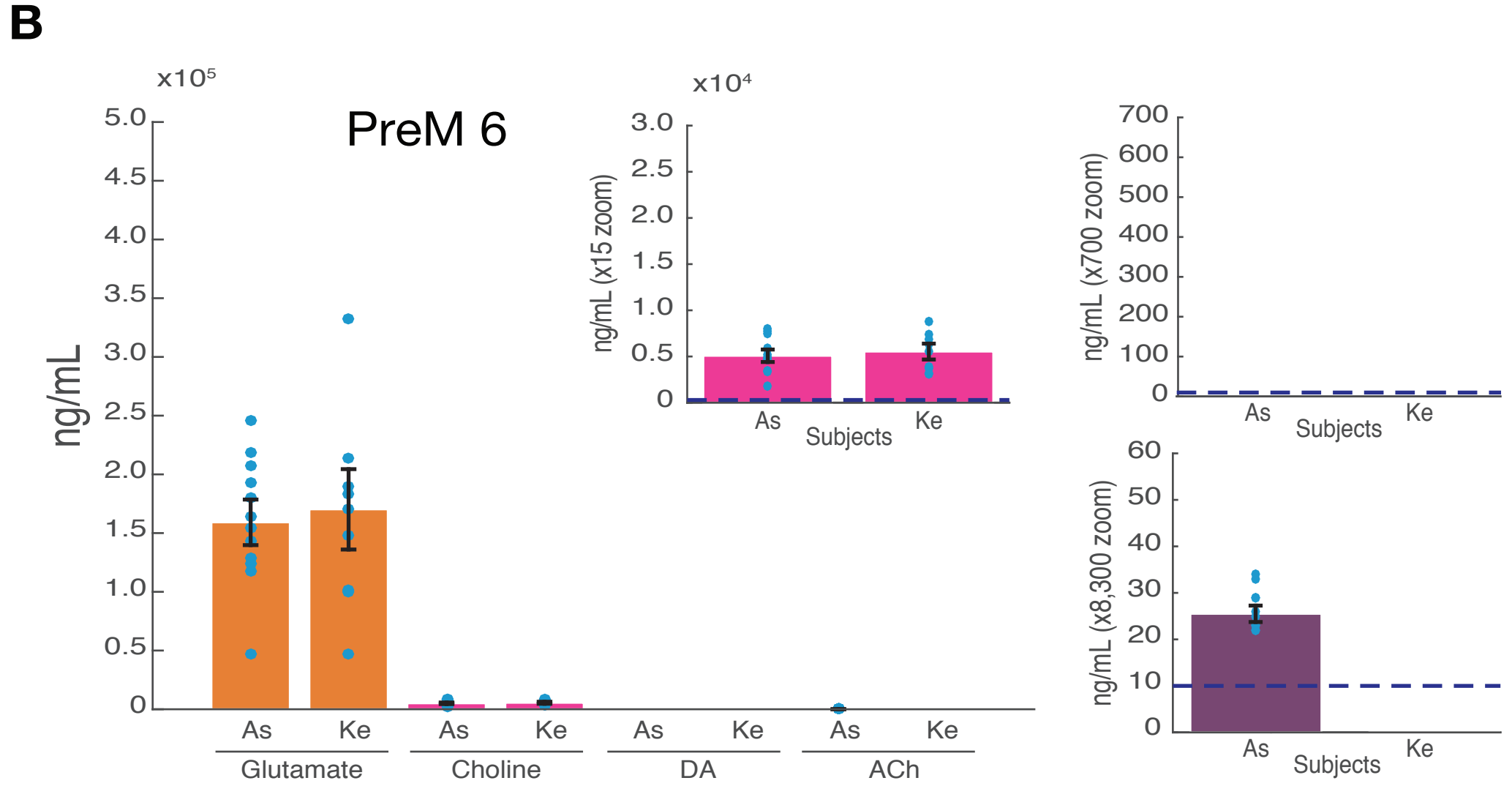
B
PreM 6
x10⁵
ng/mL
5.0
4.5
4.0
3.5
3.0
2.5
2.0
1.5
1.0
0.5
0
As
Ke
Glutamate
Choline
DA
ACh
x10⁴
ng/mL (x15 zoom)
Subjects
ng/mL (x700 zoom)
ng/mL (x8,300 zoom)

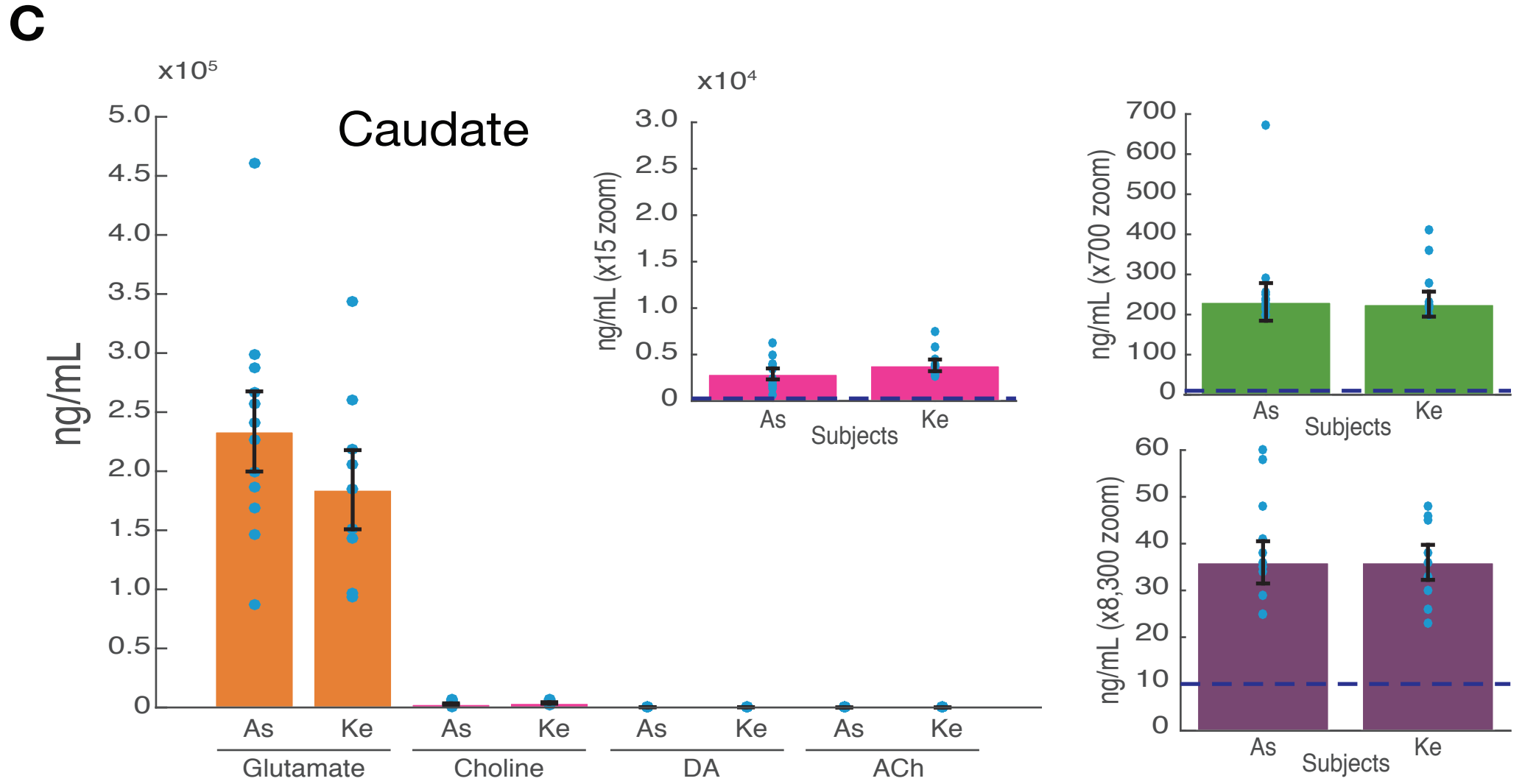
C
Caudate
x10⁵
ng/mL
5.0
4.5
4.0
3.5
3.0
2.5
2.0
1.5
1.0
0.5
0
As
Ke
Glutamate
Choline
DA
ACh
x10⁴
ng/mL (x15 zoom)
Subjects
ng/mL (x700 zoom)
ng/mL (x8,300 zoom)

Supplementary Methods

Chemicals, Reagents and Materials

The LC-MS-grade solvents methanol (MeOH), acetonitrile (ACN), isopropanol (IPA) and water, as well as the acetylcholinesterase inhibitor phenylmethylsulfonyl fluoride (PMSF) were purchased from Fisher Scientifc. Formic acid, polyacrylonitrile (PAN), N,N-dimethylformamide (DMF) and the standards of neurotransmitters: γ-aminobutyric acid (GABA), glutamic acid (Glu), acetylcholine (ACh), histamine (Hist), serotonin (5-HT), dopamine (DA) and choline (Cho) as well as their deuterated analogues were purchased from Millipore Sigma (Oakville, ON, Canada). Epinephrine (Epi), norepinephrine (NE) and their deuterated analogues were obtained from Cerilliant Corporation (Round Rock, TX, USA). Choline-D9, was purchased from Cambridge Isotope Laboratories (Tewksbury, MA, USA). The reagents used for synthesis of hydrophilic-lipophilic balance polymer particles functionalized with strong cation exchange groups, as well as compounds for preparation of PBS were purchased from Millipore-Sigma. The stainless steel wire (stainless steel grade AISI 304, 150 µm diameter) used for manufacturing of SPME probes was purchased from Unimed S.A. (Lausanne, Switzerland). The stainless steel tubing used as guiding cannulas (270 µm O.D.; 200±5 µm I.D.) was obtained from Vita Needle (Needham, MA, USA).

LC-MS/MS Analysis

On the day of analysis, the SPME probes were defrosted and desorbed into 40 µL of water/ACN/MeOH 40:30:30 (v/v/v) mixture containing 1 % of formic acid and a mixture of deuterated isotopologues of targeted neuromodulators (used as internal standards, IS) at 20 ng/mL. The desorption was carried out for 1 h with agitation at 1500 rpm. The extracts were injected into the LC-MS system for targeted neurotransmitter analysis within a few hours after desorption. All experiments were carried out using an Ultimate 3000RS HPLC system coupled to TSQ Quantiva triple quadrupole mass spectrometer (Thermo Fisher Scientific, San Jose, California, USA). Data processing was performed using Thermo software Xcalibur 4.0 and Trace Finder 4.1. For chromatographic separation of the target compounds, a modified method of what is previously reported (Cudjoe and Pawliszyn 2014) was used, adjusted to include more targeted neuromodulators and their corresponding IS. A Kinetex® PFP LC column (100 x 2.1 mm, 1.7 µm; Phenomenex, Torrance, CA, USA) was held at 30°C with the mobile phase flow rate at 400

µL/min. The mobile phase A consisted of water/MeOH/ACN 90:5:5 (v/v/v) with 0.1 % formic acid, and mobile phase B was ACN/water 90:10 (v/v) with 0.1% of formic acid. The chromatographic gradient was applied starting from 100% B for 1 min and increasing the aqueous mobile phase A to 100% for 3 min with convex gradient function, held for 0.5 min and subsequent linear return to initial conditions and re-equilibration for 1 min, yielding total time of 6.5 min. The injection volume was 10 µL. MS/MS analysis was performed with electrospray ionization in positive mode under selected reaction monitoring conditions, with two MS/MS transitions for each neuromodulator (quantifier and qualifier) and one for each IS.

Quantitation of neuromodulators

Individual stock standard solutions of all targeted neuromodulators were prepared in methanol or water with 0.1% formic acid at a concentration of 1 mg/mL and stored at −80 °C for maximum of one month. In order to calculate the amounts of neuromodulators extracted by each probe, calibrator standards prepared in the same desorption solvent as real samples were analyzed in the same batch. This instrumental calibration curve was prepared in the range of 0.1-200 ng/mL by a serial dilution of the stock standard mixture of all compounds at 1µg/mL. The IS concentration was kept constant at 20 ng/mL in all calibrators, identically as in the real samples. The amounts extracted were calculated based on linear regression equation obtained from the analytical signal (the ratio of chromatographic peak areas of analytes and their corresponding IS) plotted against the concentration.

In order to calculate the concentrations of neuromodulators in brain, matrix-matched external calibration approach was used. The surrogate matrix consisted of 2% agar gel mixed with brain homogenate in the ratio 1:1 (*v/w)*. The homogenized brain tissue was earlier incubated with 1 mM PMSF for 1 h at 37°C to prevent enzymatic digestion of acetylcholine in the calibrator samples. Due to several target compounds being present in brain homogenate at high concentrations (e.g. for glutamate and choline the “blank” brain homogenate matrix doesn’t exist), their quantitation was based on signals of their deuterated isotopologues. The calibrator samples were prepared in the surrogate matrix with concentrations of neuromodulators ranging from 5 to 3000 µg/mL for the isotopically labelled compounds or from 10 to 2000 ng/mL for the remaining compounds.

The extractions were carried out with SPME probes manufactured and pre-treated identically to the probes used for *in vivo* sampling and using the same 20 min extraction time and desorption conditions as for the real samples. The amounts of neuromodulators extracted from the calibrator samples were determined in the same way as described above and plotted against concentrations of calibrators. The resulting weighted linear regression equations were applied to the amounts of neuromodulators extracted from the *in vivo* samples, yielding values of concentrations of the compounds of interest in brain.

The limits of detection (LOD) were estimated as the levels corresponding to the signal to noise ratio of 3 and were calculated based on the signal of blank calibrator sample (considered as the noise).

Supplementary Figures

Fig S1. Behavioral task that the monkeys were engaged in. Briefly, the monkey was expected to fixate a central fixation point until criterion when two graded stimuli appeared. The graded stimuli acquired color and motion, of the graded stripes, features in either order. The two stimuli then either simultaneously dimmed (go-signal), or dimmed one at a time in either order. The monkey, through trial and error, identified the rewarded stimulus via its color feature which was the sole identifying feature informative of reward. The monkey was then expected to wait until the dimming of the selected stimulus and respond in the same direction as the motion of the graded stripes on the chosen stimulus. If the monkey correctly accomplished this, it would receive deterministic reward in the form of liquid juice. Monkey As was engaged in a variation of this task with reduced complexity in order to match monkey Ke in performance and reward acquisition over the sampling period. Figure reproduced from Hassani et al., 2017.

Fig S2. Experimental procedure from SPME probe fabrication to quantitation. Fabrication described the in-house procedure to prepare SPME probes. Preparation describes experimental set-up. Sampling describes the actual data collection process. LC/MS analysis describes the chemical quantitation of collected data samples.

Supplementary Tables

Table S1. Overview of in vivo neurochemical measurement methods

	PET imaging	**Electro-chemistry**	**Micro-dialysis**	**Solid phase micro-extraction**
Temporal Resolution	Minutes	Highest (millisecond range)	1-30 minutes; dependent on MS sensitivity, target etc.	<5-30 minutes; dependent on MS sensitivity, coating thickness, target etc.
Spatial Resolution	Voxel	High; surface area may vary (relevant for enzyme based methods)	Diffusion based; surface area may vary	Diffusion based; surface area may vary
Sensitivity	Indirect measurement via competitive radiolabeled species	High	Depending on post-hoc methods (i.e. MS)	Depending on post-hoc methods (i.e. MS)
Neuro-active targets	A few at most	A few at most	Many	Many
Non-neuro-active targets	No	No	Yes, greater efficacy for hydrophilic compounds	Yes, greater potential efficacy for hydrophobic compounds
In vivo feasibility	Difficult in awake, behaving animal models; movement highly restricted	Good (low reliability in NHPs)	Good, often requires chronic implant of cannula for repeated measurements	Very good; robust placement of multiple simultaneous probes and repeatable acute measurements
Cost	High	Requires special equipment	Requires special equipment	Easy to port to an acute micro-electrode setup; requires a chemistry core

Table S1. A comparison of methods capable of measuring single or multiple neurochemicals in vivo. Temporal resolution, spatial resolution, sensitivity, capability to measure neuro-active and non-neuro-active compounds, in vivo feasibility and cost. PET: positron emission tomography; NHP: non-human primate; MS: mass spectrometer.

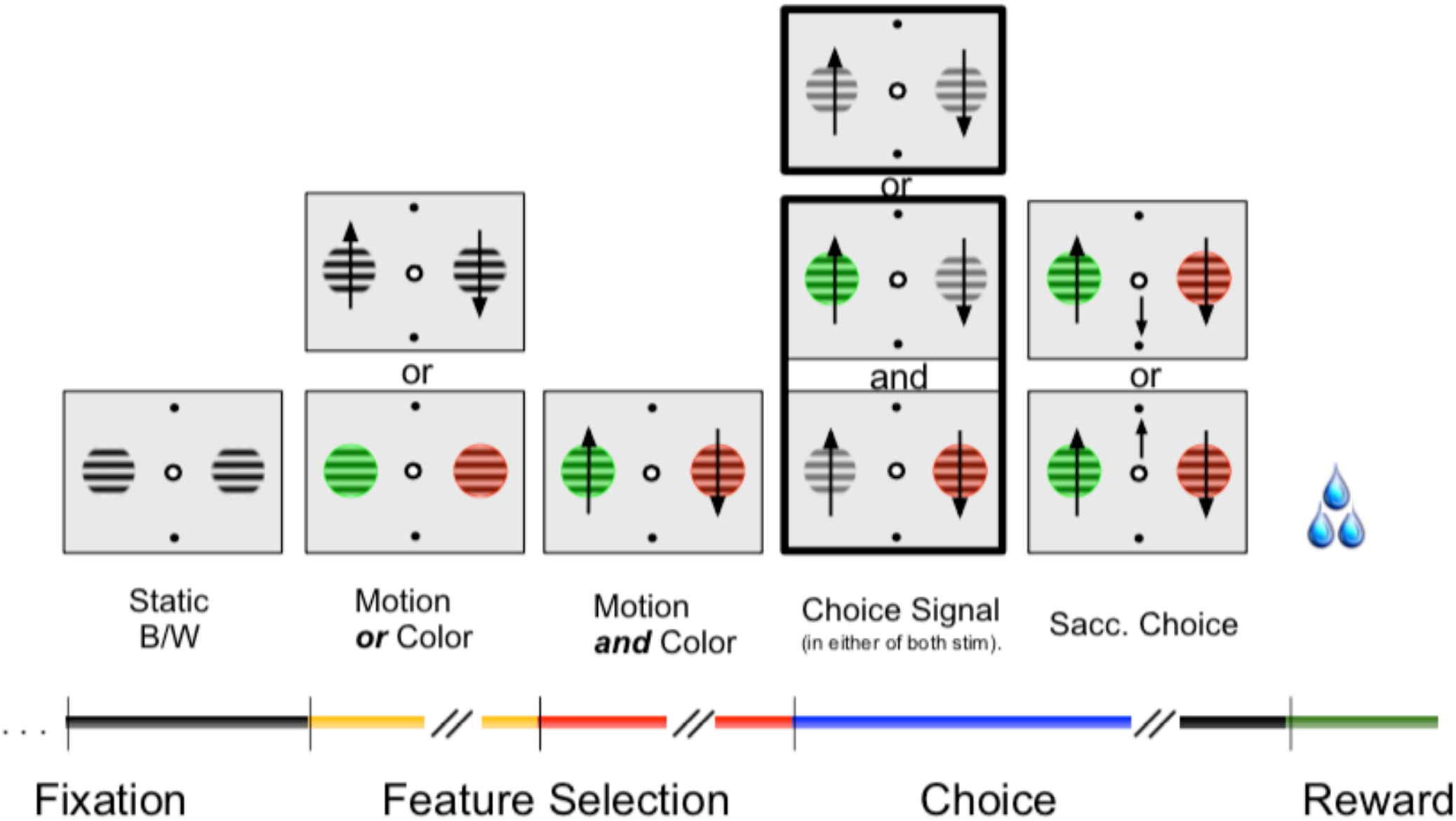
or
or
and
or
Static
B/W
Motion
or Color
Motion
and Color
Choice Signal
(in either of both stim).
Sacc. Choice
Fixation
Feature Selection
Choice
Reward

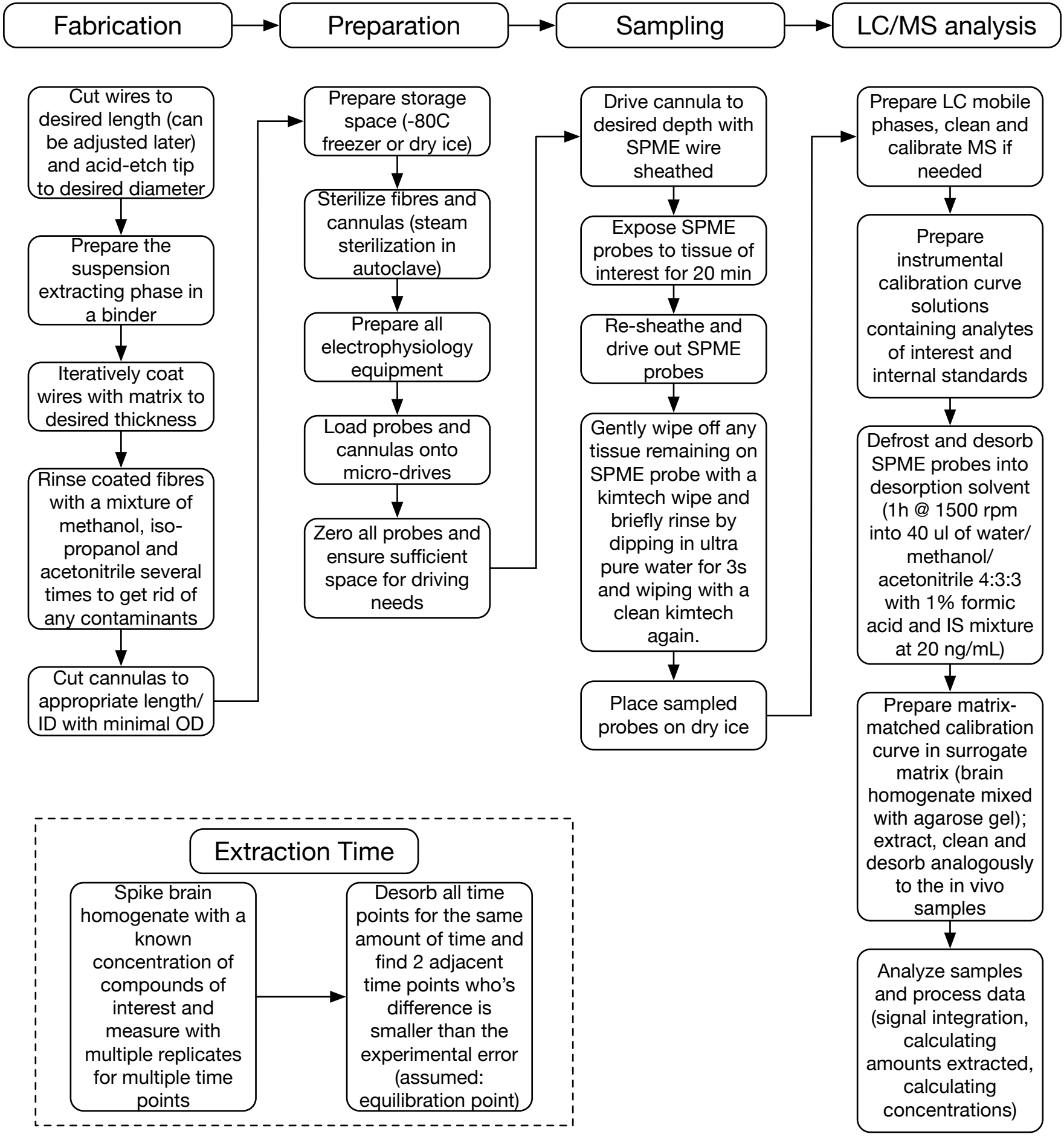
Fabrication
Preparation
Sampling
LC/MS analysis
Cut wires to desired length (can be adjusted later) and acid-etch tip to desired diameter
Prepare the suspension extracting phase in a binder
Iteratively coat wires with matrix to desired thickness
Rinse coated fibres with a mixture of methanol, iso-propanol and acetonitrile several times to get rid of any contaminants
Cut cannulas to appropriate length/ ID with minimal OD
Prepare storage space (-80C freezer or dry ice)
Sterilize fibres and cannulas (steam sterilization in autoclave)
Prepare all electrophysiology equipment
Load probes and cannulas onto micro-drives
Zero all probes and ensure sufficient space for driving needs
Drive cannula to desired depth with SPME wire sheathed
Expose SPME probes to tissue of interest for 20 min
Re-sheathe and drive out SPME probes
Gently wipe off any tissue remaining on SPME probe with a kimtech wipe and briefly rinse by dipping in ultra pure water for 3s and wiping with a clean kimtech again.
Place sampled probes on dry ice
Prepare LC mobile phases, clean and calibrate MS if needed
Prepare instrumental calibration curve solutions containing analytes of interest and internal standards
Defrost and desorb SPME probes into desorption solvent (1h @ 1500 rpm into 40 ul of water/ methanol/ acetonitrile 4:3:3 with 1% formic acid and IS mixture at 20 ng/mL)
Prepare matrix-matched calibration curve in surrogate matrix (brain homogenate mixed with agarose gel); extract, clean and desorb analogously to the in vivo samples
Analyze samples and process data (signal integration, calculating amounts extracted, calculating concentrations)
Extraction Time
Spike brain homogenate with a known concentration of compounds of interest and measure with multiple replicates for multiple time points
Desorb all time points for the same amount of time and find 2 adjacent time points who's difference is smaller than the experimental error (assumed: equilibration point)